GENESIS OF UNIQUE CARBONATE FANS IN A PRE-SALT RESERVOIR ANALOG, INDIO MOUNTAINS, WEST TEXAS

ANDRE ARMANDO LLANOS

Master's Program in Geology

APPROVED:

Benjamin Brunner, Ph.D., Chair

Katherine Giles, Ph.D.

Jerry Johnson, Ph.D.

Charles Ambler, Ph.D.
Dean of the Graduate School

DEDICATION

This thesis is dedicated to Cally, my wife.

For Geology is the study of pressure and time, yet… time is love.

GENESIS OF UNIQUE CARBONATE FANS IN A PRE-SALT RESERVOIR ANALOGUE, INDIO MOUNTAINS, WEST TEXAS

by

ANDRE ARMANDO LLANOS, B.S.

THESIS

Presented to the Faculty of the Graduate School of

The University of Texas at El Paso

in Partial Fulfillment

of the Requirements

for the Degree of

MASTER OF SCIENCE

Department of Geological Sciences

THE UNIVERSITY OF TEXAS AT EL PASO

December 2017

ACKNOWLEDGEMENTS

I would like to express my gratitude and sincerest appreciation to my wife, Cally, whom has endured this entire process at my side while I pursued my Geology B.S. and M.S Degrees from UTEP for the past five years. I would not be in this fortuitous position without her enduring support, unparalleled patience, and her agreeing to go on a first date geology field trip around Austin provided by my Intro to Geology class at UT Austin. I would like to thank my brother, sister, and especially my mother for pushing me to pursue my love of rocks and geology while that passion was in the early stages of educational infancy. I would like to thank the biggest rock known only to my family, my loving and sweet Mama Goya, whom provided my aunts, uncles and cousins (who I spent the majority of time with growing up in El Paso), her infinite wisdom, support and faith and as a consequence, I would simply not be the person I am today without her and all of them.

In December of 2014, Dr. Benjamin Brunner agreed to be my master's thesis advisor and through the years has provided far more than that role. I cannot express enough how thankful I am for his unyielding wisdom, guidance and mentorship that I received throughout this unprecedented journey. Thanks Ben. Additionally, I wish to thank Dr. Gail Arnold for her kindness, providing an open ear, offering advice for personal and educational challenges, and a reliable cup of coffee. Special thanks to Dr. Katherine Giles and ITS for their support and attention to my research. This work would not have been possible without access to the Indio Mountains Research Station headed by Dr. Jerry Johnson who is also serving as my committee member. Thank you Jerry for your guidance out at the Indio Mountains.

Finally, thank you to Eddie, our Jack Russell Terrier. He has been our fur child for 2 years and counting but brings an unsurpassable amount of joy to his mother Cally and I.

ABSTRACT

Hydrocarbon exploration in pre-salt sediments of rift basins on the South Atlantic Margin have proven to be successful major oil plays. Located on the western margin of the rift, the Brazilian pre-salt reservoirs of the Santos, Campos, and Espirito Santo Basins are hosted by lacustrine/marine-influenced carbonates that comprise laterally extensive, laminated microbialite facies. The Indio Mountains, located in West Texas, provide well-exposed outcrops of Lower Cretaceous marine and non-marine rift basin strata that can be considered a reservoir-analog to the South Atlantic Margin pre-salt facies. Of particular interest for hydrocarbon exploration are unique carbonate features that have been discovered in the Lower Cretaceous Yucca Formation at the Indio Mountains. The carbonate features include a laterally continuous bed of septarian nodules and radial carbonate fans that are associated with fault zones. Field observations show that syndepositional faulting took place during the deposition of the lake sediments and fluvial deposits. The lakes of the Upper Yucca Formation were exposed to strong evaporation, and were supplied with water by rivers and groundwater discharge, as well as by fluids entering the lakes via fault systems. These conditions maintained alkaline lake conditions which in concert with oxidation of biogenic methane at the seabed favored carbonate precipitation.

The presence of radial carbonate fans indicates the presence of syndepositional faults that could affect the interconnectedness of otherwise compartmentalized reservoir blocks, whereas the clay-rich lake sediments point the strong possibility that thin lake beds, which may not be resolvable by seismic methods could act as impermeable seals, causing compartmentalization. As such, the lacustrine sediments form the Upper Yucca Formation are the key to so far untapped information about the geologic history of pre-salt sedimentary deposits, and their propensity to become hydrocarbon reservoirs.

TABLE OF CONTENTS

LIST OF FIGURES

1. INTRODUCTION

1.1 PRE-SALT HYDROCARBON RESERVOIRS

The discovery of vast hydrocarbon reservoirs and successful production along the South Atlantic margin (Figure 1; Text Box 1) has generated great interest in understanding the depositional environments and the diagenetic history of these oil fields. Ultra deep-water fields are currently exploited in the Campos basin and the gained expertise and improved technology are adapted to wells in the Santos basin, some of which are targeting carbonate reservoirs sealed beneath a thick evaporite layer (Beasley et al., 2010). These petroleum reservoirs are referred to as Pre-Salt plays due to their stratigraphic position as packages of sedimentary rocks, which are overlain by a thick cover of evaporite deposits. The Pre-Salt plays of the Central Segment in Brazil originated from syn-rifting cycles of the Gondwana continental break-up, which formed basins that were infilled with organic-rich lacustrine black shales, and fluvial deltaic sediments (Blaich et al., 2011; Marcano et al., 2013). These sediments are the source rocks for Pre-Salt petroleum systems in The Campos, Lower Congo, Colorado, and Orange basins.

TEXT BOX 1: "The presalt play, founded on the Tupi in the Santos Basin, is pushing technological boundaries as E&P teams seek to define its geographic limits. Containing potential recoverable volumes of 795 million to 1.3 billion m^3 [5 to 8 billion bbl] of oil equivalent, the Tupi structure is just one of several found beneath a thick layer of salt." (Beasley et al., 2010)

1.2 CHALLENGES IN THE EXPLORATION OF PRE-SALT PLAYS

1.2.1 Ultra-deep water offshore location

The Pre-salt petroleum systems in the South Atlantic are predominantly found offshore, some ranging out to 300 km off the coast of Brazil (Beltrao et al., 2009). Moreover, the hydrocarbons are often recovered from ultra-deep waters. The Tupi oilfield for example, lies under 2,126 m [6,975 ft] of water in the Santos Basin. The remoteness of these locations, combined with the challenges of drilling in ultra-deep waters and fluctuating oceanic conditions pose massive technical and logistical challenges for drilling at such sites (Beasley et al., 2010). Consequently, construction of drilling platforms offshore is extremely costly and failure to reach the target can be financially catastrophic.

1.2.2 Exploration Target Buried Under Thick Evaporite Deposits

Salt deposits covering Pre-salt plays often range from 2,000 m to 3,000 m (Beltrao et al., 2009; Beasley et al., 2010) in thickness. Drilling through these sediments not only adds to the technical challenges caused by the remote deep-water location of Pre-salt reservoirs, but also hampers seismic imaging, a key technology in hydrocarbon exploration. The presence of the salt cover negatively affects the seismic resolution that can be achieved for the underlying sediments. Typically, seismic resolution on a bed of less than 25 m is very poor because the top and the base reflectors cannot be resolved (Chopra et al., 2006). The required deep seismic penetration and additional noise caused by extremely high seismic contrasts between salts and other sediments make it difficult to retrieve such a high seismic resolution and to obtain reliable, interpretable seismic data in general.

1.3 NEED FOR ACCESSIBLE PRE-SALT RESERVOIR ANALOGUES

In light of the high financial risks related to the exploration of Pre-salt reservoirs, there are expensive and technical challenges in the retrieval of sediment cores. Adding to these expenses are the fact that seismic imaging may not yield a resolution that is sufficient to identify critical structures such as sediments beds of variable thickness and those that are less than 50m in thickness. Therefore, there is an urgent need to find other approaches to accurately interpret and/or predict Pre-Salt plays. Accurate characterization of Pre-Salt reservoirs through outcrop analogue studies becomes vital to exploration and production efforts, as there are significant gaps in industry knowledge regarding their depositional environments and subsequent diagenetic processes (Beasley et al., 2010).

1.3.1 Criteria for Suitable Analogues for South Atlantic Pre-Salt Deposits

It is generally accepted that the Pre-Salt deposits in the South Atlantic formed during the Early Cretaceous as a result of extensional tectonics related to the opening of the South Atlantic (Figure 2). Due to uplift related to the Tristan da Cunha hotspot, subsidence was slowed down, resulting in continental rather than marine depositional environments (Beasley et al., 2010). This information is helpful in the search for suitable analogues, as it provides insights into the climatic conditions and tectonics, the key controls on sedimentology, geometry and structure of Pre-salt deposits.

Tectonic settings determine the rates of subsidence and sedimentation that can influence the patterns of continental drainage and the location of clastic sediment input (Platt and Wright, 1991). Moreover, tectonics also control the formation of structural elements such as faults and folds that often play a critical role in hydrocarbon exploration. Climate impacts the rate and nature of primary productivity, influences the chemical weathering, erosion, and sedimentation rates of

the catchment area, and thus determines the supply of detritus as well as dissolved constituents, such as carbonate to the depositional environment (Platt and Wright, 1991). Last but not least, an appropriate analogue for Pre-salt sediments in the South Atlantic should mirror the lithological content of reservoirs that have been drilled to this point.

In summary, the 'right' analogue for Pre-Salt sediments from the South Atlantic should have the same 1) climate – i.e. global greenhouse conditions that prevailed during the Early Creataceous 2) tectonic setting – i.e. extensional basins, 3) subsidence history – i.e. continental sedimentation rather than marine transgression, and 4) lithological content – i.e. lake carbonates.

1.3.2 Previous Analogue studies for South Atlantic Pre-Salt Reservoirs

Previous analogue studies heavily relied on lithological content as criterion, in particular the finding of microbial carbonates in such settings (Text Box 2). Carbonate hydrocarbon reservoirs of microbial origin have been reported from the Cretaceous (Aptian) South Atlantic rift-sag basins. Carbonates with similar textures have been described in the Campos Basin, off-shore Brazil by Dias (2005) and also in the Barra Velha Formation, Santos Basin by (Terra et al., 2010). These carbonates have been classified as 'Pre-Salt microbialites' that developed before the main phase of salt deposition within the sag basins. These findings have triggered intense research by academia and the petroleum industry to search for possible Pre-Salt microbialites analogues that will further the understanding of these intractable rocks and their complex pore systems (Bosence et al., 2015).

1.3.3 Challenges with Previous Pre-Salt Analogue Studies

So far, the focus of microbialite studies are either on marine settings (Jahnert and Collins, 2011; Hamon et al., 2012; Jahnert and Collins, 2012; Droxler et al., 2014), which are not

comparable to lacustrine systems, or on lacustrine environments during icehouse climate conditions, e.g. the Eocene Green River Formation (Seard et al., 2013; Awramik and Buchheim, 2012). This is problematic for several reasons. Among many of the carbonate formations that are being exploited for petroleum recovery, a comparative study shows that the facies models and cycle stratigraphy for microbialite carbonates are inconsistent relative to another and differ significantly (Wright and Barnett, 2015). For example, a closer look at the Barra Velha Formation, which is a unit that is part of the Santos Basin Presalt reservoir, reveals that these deposits are of lacustrine rather than marine origin. This argument is based on the absence of typical marine fossils and the absence of early sulfate minerals such as gypsum and anhydrite suggesting that these particular carbonates were not sourced from marine waters. The microscopic textures of sedimentary rocks from the Barra Velha Formation vary widely and are not typical for what has been reported from modern and fossil microbialites (Monty and Hardie, 1976; Flügel, 2010;

TEXT BOX 2: Microbialites

Recent findings have led researchers to believe that microbes are the primary drivers for lacustrine carbonate production in Pre-Salt petroleum systems. Microbialites are organosedimentary deposits formed from interaction between benthic microbial communities and detrital or chemical sediments. These communities trap and bind detrital sediments and form various features such as boundstones, tufa, and framestones (Burne and Moore, 1987.) Microbial activity can mediate the precipitation of carbonates in lacustrine or marine environments. Because some microbes (e.g. halophiles) have the ability to thrive where other competing organisms do not, the formed carbonates can become the dominant sedimentary rocks. This is for example the case for stromatolites in highly saline environments found in the Great Salt Lake, Utah, or Shark Bay, Australia and for layered microbialites in light deprived coral reefs around the world (Heindel et. al., 2012). Notably, carbonate precipitation that leads to the formation of similar structures can also occur in absence of microbial activity (abiotically).

Riding, 2008; Wright and Barnett, 2015). It is more likely that the found cementstones are abiotic precipitates than of microbial origin (Terra et al., 2010; Bosence et al., 2015).

In general, the microbialite carbonates that have been identified in the South Atlantic Pre-salt deposits are interpreted to have formed in highly alkaline lakes under a greenhouse climate (e.g. Dorobek et al., 2012). This is in stark contrast to current microbialite studies from marine settings (e.g. Jahnert and Collins, 2011; Hamon et al., 2012; Jahnert and Collins, 2012; Droxler et al., 2014), and studies from lacustrine environments during icehouse climate conditions (e.g. Eocene Green River Formation (Awramik and Buchheim, 2012; Seard et al., 2013), which are drastically different from greenhouse conditions that influence the establishment and growth rates of carbonates similar to the South Atlantic Pre-Salt Plays.

Tectonics and mixed siliciclastic-carbonate lacustrine sediments

While lacustrine microbialites are certainly an important facies in Pre-salt reservoirs, they are only one component of a far more complex system. Pre-Salt plays are a product of interminably slow tectonic and depositional processes involving continental rifting, seafloor spreading and sedimentation of continental clastics. The initial phase of the continental breakup is referred to as the syn-rift cycle (Marcano et al., 2013). Crustal stretching within the syn-rift cycle creates faulting and fracturing networks that are thought to provide pathways for delivering fluids that promote diagenetic processes, especially mineral dissolution, which not only improve the reservoir quality by connecting porosity networks (Beasley et al., 2010) but also sets up the framework for abiotic carbonate production near these fault zones.

1.3 IMPLICATIONS FOR RESEARCH ON PRE-SALT RESERVOIRS

Due to the high risks and costs associated with drilling in Pre-salt reservoirs and the limitations in seismic resolution of these deposits, the study of Pre-salt analogues is key to

hydrocarbon exploration. Good analogues provide a match for the climate and tectonic setting as well as for the sediment types that predominate in such systems. Analogue studies that have been carried out so far have often focused on individual components – particularly microbialites – of a much more intricate system. Considering that: a) abiotically precipitated carbonates and mixed carbonate-siliciclastic lacustrine sediments are important components of Pre-salt deposits and b) faults and fracture networks are key elements of hydrocarbon plays it is evident that the so far narrow focus on microbialite analogues must be widened to a much broader view that encompasses the full spectrum of sedimentary and structural features relevant for South Atlantic Pre-salt plays. The Indio Mountains in West Texas provide an exceptionally well-exposed, laterally continuous outcrop of Lower Cretaceous lacustrine rift-basin strata (Figure 3; Underwood, 1962; Haenggi, 2002; Page, 2011) that can be used to address the aforementioned issues with current analogue studies.

2. GEOLOGIC SETTING

The Indio Mountains provide an outcrop analogue to Pre-Salt reservoirs that sets it apart from other sites that have been used to investigate the depositional and diagenetic history of Pre-Salt sediments. Located in West Texas along the US-Mexico border, approximately 200 km southeast of El Paso, they form the southern extension of the north-northwest-trending Eagle Mountains and terminate to the south at the Rio Grande River. Among other strata, the range contains well exposed sediments of the Lower Cretaceous that were deposited on the eastern margin of the Chihuahua Trough (Figure 4; Underwood, 1962; DeFord, 1964). The Chihuahua Trough is a Mesozoic rift basin trending northwest-southeast and is bounded by the Diablo platform to the northeast and the Aldama platform to the southwest in Mexico (Haenggi, 2002). Chihuahua Trough extension began during Middle Jurassic forming the Proto-Gulf of Mexico. The extension is likely related to the opening of Atlantic Ocean. Subsequent Laramide-age (Late Cretaceous to Eocene) crustal shortening locally inverted the strata of the Chihuahua Trough (Bird, 1998). This thrust inversion placed Chihuahua Trough rift strata over Precambrian and lower Paleozoic rocks of the adjacent Diablo platform. In the Indio Mountains, only the Lower Cretaceous rocks of the eastern Chihuahua trough are exposed within three Laramide-age thrust sheets (Figure 3; Page, 2011).

2.1 THE YUCCA FORMATION

Carbonates found within the Yucca Formation provide a potential analogue to the deposition of lacustrine Pre-Salt deposits along the Central South Atlantic margin. This formation is informally subdivided into two members based on an abrupt change in sediment texture. The Lower Member dominantly comprises coarse-grained, conglomerate rich siliciclastic alluvial and

fluvial facies. The Upper Member consists of finer grained conglomerate, sandstone, siltstone, mudstone, and lacustrine to marginal marine limestone. The boundary between the two members is identified by an abrupt fining upward change from very coarse grained, poorly sorted conglomerate and conglomeratic sandstone and siltstone interbedded with thin limestone (Figure 4, 5; Underwood, 1962). The Yucca Formation is part of the syn-rift sequence of the Chihuahua Trough, which is transgressively overlain by shallow-marine carbonate strata of the Bluff Mesa Formation (Underwood, 1962; Haenggi, 2002). The Upper Member of the Yucca Formation is the focus of this study, as it represents a setting that can be considered to be an appropriate analogue to Pre-Salt mixed clastic lacustrine sediments that were deposited in an extensional regime and that were subsequently overlain by marine transgressional strata.

2.1 PREVIOUS STUDIES IN THE YUCCA FORMATION

Initial investigations revealed that the geometry and lithology of the Yucca Formation is heavily affected by syndepositionary faults (Li, 2014). Along the faults of the Upper Yucca are unique carbonate features that were documented by Li (2014). These carbonate features include laterally continuous beds of septarian nodules – informally referred to as 'potato-beds' – and radial, fan-shaped carbonates that appear to only occur in close proximity to the faults. This finding leads to the conclusion that at least the genesis of the fan-shaped carbonate is linked to the presence of syndepositional faults, whereas a similar connection for the septarian nodules remains speculative. Field reconnaissance has revealed that the radial carbonate fans are only found near the syndepositional faults located in Echo Canyon, a region that is characterized by several major faults. Establishing a geochemical understanding of the highly localized connection between faults and fan-shaped features, as well as the bedding surfaces abundant with carbonate septarian concretions is the primary object of this research.

3. HYPOTHESIS

Based on the preliminary observations, I formulate the following hypothesis:

TEXT BOX 3: Hypothesis

The interplay between tectonics and climate is responsible for the formation of the great variety of lacustrine-fluvial sedimentary features in the Yucca Formation. Faults and climate variability are the cause for the high diversity on decameter scale. Driving factors for small scale features such as potato beds and carbonate fans are fluid flow along faults combined with high alkalinity caused by arid conditions, as well as stratification of the water column in paleo-lakes.

3.1 HOW THE STUDY OF THE GEOLOGY OF THE INDIO MOUNTAINS WILL FURTHER THE UNDERSTANDING OF PRE-SALT PLAYS

The paloeogeographic, paleoclimatologic and tectonic setting make the Indio Mountains an analogue of Pre-salt reservoirs. The richness in sedimentary facies and structural features, such as the syndepositional faults found at this location have a high potential to offer new insights into geology of Pre-salt deposits.

3.2 HOW THIS STUDY WILL IMPROVE GENERAL KNOWLEDGE ABOUT PRE-SALT PLAYS

The Indio Mountains allows for an accurate characterization of fluvial/deltaic mixed siliciclastic and lacustrine systems that reflect the Cretaceous climatic conditions and extensional tectonics of the Pre-Salt plays in the South Atlantic. This broader view enlarges the inventory of Pre-Salt features beyond what is known from studies of microbialite dominated systems. In particular, we will: 1) gain insight into the richness of sedimentary facies, and their qualities as reservoir rocks, 2) elucidate if abiotic carbonate features (i.e. carbonate fans and septarian concretions) that can be misconstrued as microbialites are abundant in lacustrine Pre-Salt deposits,

3) answer the question if syndepositional faults can positively or negatively affect the interconnectiveness of Pre-Salt reservoir strata, 4) understand if diagenesis related to fluid flow along faults causes occlusion of primary porosity and decrease in permeability and/or generation of secondary porosity and 5) quantify the abundance of syndepositional faults. These insights, which are critical for hydrocarbon exploration, will allow for the establishment of more accurate conceptual models for Pre-Salt plays.

3.3 How This Study Will Help Specific Oilfield Exploration: Diagnostic Carbonate Features

If our hypothesis that there is an intimate relationship between radial carbonate fans, potato-bed forming septarian concretions and syndepositional faults is correct, this knowledge will be advantageous in oilfield drilling operations. If such carbonate features are retrieved during drilling, the operators would be able to conclude that the bore hole is in proximity to a syndepositional fault that once acted as conduit for fluids. These diagnostic features will allow the exploration team to better predict the reservoir quality and potential variability in the vicinity of the bore hole, and to address potential challenges, such as drilling hazards, at an early stage.

3.4 Arising Questions

Based on predictions about how investigating the Yucca Formation in the Indio Mountains will improve the understanding of Pre-salt reservoirs I formulate the following questions:

TEXT BOX 4: Arising questions

Q1) What is the abundance of syndepositional faults?

Q2) Does the network of faults act as a seal or a conduit?

Q3) How abundant are carbonate fans and beds of septarian concretions?

Q4) Is there a link between carbonate features and faults?

4. OBJECTIVES

4.1 DETERMINE ABUNDANCE OF SYNDEPOSITIONAL FAULTS

Rationale: Faults are key elements of reservoir systems, because they can act as a conduit or as a seal for migrating hydrocarbons but also serve as a formations ability to fracture and become reservoirs (Figure 6). For these reasons, it is important to obtain an overview on how abundant syndepositional faults are in Pre-salt deposits.

Action: Extensive mapping of the Echo Canyon area. Echo Canyon owes its existence to a fault that establishes canyon drainage and erosional pathways, and which are associated with syndepositional faults that are splayed throughout an area of $1km^2$. To date, no detailed maps of the Upper Yucca formation are available for the region SSE of Echo Canyon. Mapping of this area is vital for this study as there may be additional outcrops of the carbonate fans that are associated with syn-rift faults. Currently there is no evidence of syndepositional faulting near Squaw Canyon. Therefore, the focus of this study is on Echo Canyon.

4.2 ASSESS IF SYNDEPOSITIONAL FAULTS ACT AS SEAL OR CONDUIT

Rationale: Fluid flow along faults can cause precipitation of new mineral phases that may act as seals for hydrocarbon migration (e.g. carbonate cements), but can also induce leaching and dissolution of existing phase, creating secondary porosity and open fluid pathways. Moreover, depending on the P-T regime at which faulting occurred, the faults may act as seals (e.g. fine-grained, impermeable fault zone) or conduits (e.g. open fractures due to brittle deformation) (Figure 6). For the interpretation of Pre-salt deposits and their reservoir properties, it is crucial to know which scenario – seal or conduit – is more realistic.

Action 1: Determine field relationships. Outcrops of syndepositional faults show varying ranges of displacement. The offset can be large enough to bring different permeable formations in contact with each other, resulting in mixing of fliud phases. Such mixing can be traced by analyzing element distribution patterns and by isotope compositions.

Action 2: Perform petrographic and geochemical analysis to determine: 1) Cementation along faults, and 2) Characteristics of what fluids have migrated through the fault.

4.3 Determine Abundance of Carbonate Fans & Beds of Septarian Concretions

Rationale: Carbonate fans and beds of septarian concretions could be diagnostic features that indicate proximity to faults and provide a detailed framework for geochemical and depositional history of the lacustrine systems in which they formed. This information would be of high importance for hydrocarbon exploration. With sufficient training, fragments of carbonate fans and septarian concretions can be identified when encountered in drilling operations. However, the question arises if these unique carbonate features are in an abundance that makes it likely that such fragments would be retrieved during drilling. To assess this potential, we need to determine how abundant these features are.

Action: Extended field reconnaissance excursions with the aim to discover more sites that exhibit 'potato beds' or septarian concretions. A focus will be on detailed mapping SSE of Echo Canyon, which so far has not been mapped in high resolution and on exploring canyons W and E of Echo Canyon that might be fault-related.

4.4 Assess if there is a link between Faults & Carbonate Features

Rationale: If there is a link between syndepositional faults and the formation of beds of septarian concretions and carbonate fans these features could be used as diagnostic tool for the presence of

faults in the vicinity of the location where the features are found. However, this hypothesis needs to be tested. To do so, we consider two different scenarios for the formation of the carbonate features. In the first scenario, beds of septarian concretions and carbonate fans are presumed to simultaneously form at different locations in a lacustrine environment in conjunction with fluid flow along syndepositional faults, whereas in the second scenario the features form at different times and unrelated to fluid flow at syndepositional faults. Either scenario is expected to leave unique geochemical fingerprints. In the first scenario there should be geochemical patterns consistent with mixing of lake water and fluids migrating along syndepositional faults. This mixing pattern will be preserved in carbonate cements of sediments in close proximity to faults, carbonate fans, and septarian nodules as mixing trends in the element and isotope distribution,

TEXT BOX 5: Geochemical patterns carbonate cements of sediments in close proximity to faults, carbonate fans, and septarian nodules

Isotopic ($\delta^{13}C_{carbonate}$, $\delta^{18}O_{carbonate}$, $\delta^{18}O_{CAS}$, $\delta^{34}S_{CAS}$, $^{87/86}Sr_{carbonate}$), chemical ($Ca_{carbonate}$, $Mg_{carbonate}$, $Sr_{carbonate}$) and mineralogical compositions will be compared to assess the influence of fluid migration through the faults and its impact on carbonate growth of septarian concretions, carbonate fans, and carbonate cements. Even though the geochemical analysis of such rock samples may indicate that the rocks formed by fluid migration through an interconnected syndepositional fault system, it does not reflect other influences on the depositional system such as the periodicity of fluvial input related to changes in climatic conditions. These factors impact the alkalinity and salinity of the lacustrine environment, and impact the geochemical zonation of the water column (i.e., disturbance of stratified water bodies by means of mixing and relative position of the mineral formation to the sediment-water interface) and the microbial activity that mediates the formation of minerals. In order to decipher these signals, and to disentangle the impact of these external factors from the imprint of fluid migration, the isotopic, chemical and mineralogical compositions of carbonate features must be compared to carbonates that are not associated with the influence of fluid interaction through fault seams.

such as strontium/calcium ratios (Sr/Ca ratios), strontium isotope composition of carbonate ($^{87/86}Sr_{carbonate}$), content as well as oxygen and sulfur isotope composition of carbonate associated sulfate (CAS, $\delta^{18}O_{CAS}$, $\delta^{34}S_{CAS}$) or carbon and oxygen isotope composition of carbonate ($\delta^{13}C_{carbonate}$, $\delta^{18}O_{carbonate}$). In the second scenario, where the carbonate features form at different times there should be no systematic patterns for the element and isotope distribution in the investigated carbonates.

Action: Perform geochemical analyses of carbonate cements of sediments in close proximity to faults, carbonate fans, and septarian nodules near Echo Canyon, which displays several faults that the carbonate radial fans appear to be associated with.

5. METHODS

To address our questions and reach my objectives, I employed the following methods: i) field work including detailed mapping, measurement of stratigraphic sections and sample collection, ii) petrographic thin section analyses, and iii) extraction of easily soluble and carbonate associated sulfate (ESS and CAS, respectively) as well as carbon and oxygen isotope analyses of Upper Yucca Formation septarian nodule samples from Squaw Canyon, Echo Canyon, and Bluff Mesa and radial fan samples from West Echo Canyon site and the newly discovered East Echo Canyon site.

5.1 FIELD WORK & SAMPLING STRATEGY

Field work for this study was accomplished in seven expeditions, one trip in September 2015, one trip in January 2016, two trips in April 2016, one trip in June 2016 (ill-advised for future consideration as the heat conditions are extraneous), one trip in December 2016, and once more in September of 2017. The first two trips served as reconnaissance expeditions, whereas the rest provided many of the key observations necessary for this study, including the discovery of the continuation of the radial carbonate fan (RCF) bed, collection of samples for petrographic and geochemical analyses, detailed mapping including stratigraphic sections, and time spent in the field with thesis advisor Dr. Benjamin Brunner.

Detailed geological maps of the study area and lithological descriptions of the geologic units were available (Page, 2011; Li, 2014; Fox, 2016). This literature provided detailed descriptions of the Lower and Upper Yucca formations, which were used for the identification of unit boundaries. Prior research by Li (2014) and Fox (2016) focused on the sedimentologic features of the Upper Yucca Formation in between of Echo Canyon road and Squaw Canyon road.

This study extended the mapped area into the Southeastern area of Echo Canyon from Echo Canyon Road (30°46'16.57"N 105°00'17.42"W, 30°45'42.56"N 105°00'03.56"W, 30°45'46.72"N 104°59'43.08"W, 30°46'36.67"N 104°59'55.00"W) using a handheld device with a georeferenced digital mapping program called Field Move Clino. A total of 50 hand samples were collected across 4 primary areas of focus in this study.

5.1.1 Field Mapping

A detailed map of the study was created (Figure 7) through extensive fieldwork that included the use of a GPS handheld phone device with a georeferenced digital mapping program called Field Move Clino, a Brunton compass to measure strike and dips of beds, and a Jacob staff to measure bed thicknesses. The phones capabilities allow for point data to be stored at a single sample location including: observation notes, photographs, and confirmation of bedding planes. The mapping program also has export capabilities where a .kmz file could be digitally moved into Google Earth or onto a georeferenced map where it could further be illustrated accurately and established.

5.1.2 Digital Mapping & 3D Modeling from Field Data

Rationale for digital mapping: To elucidate if there is a link between RFCs, syndepositional faults, and geochemical setting it is of utmost importance to identify the spatial relationships between *RFCs* and syndepositional faults. The discovery of a large number of RFCs that had previously escaped detection, and the resulting need for a re-interpretation of the motion sense at syndepositional faults at the West Echo Canyon site demonstrated that even with most careful field work, key geological elements may be overlooked with the classical field mapping approaches. For this reason, I decided to augment my field mapping by accompanying it with a bird-view

digital mapping technique. This approach not only allows to cross-reference findings based on classical field work, but also to visualize geological features in 3D.

I employed a new tool known as Structure for Motion (SfM) photogrammetry through the use of unmanned aerial systems (UAS), also known as drones. I developed a strategic flight plan to cover the area of interest with focus on structural and tectonic components that have influenced the genesis of RCFs within the Echo Canyon site. A drone flight was conducted over the Upper Yucca Formation and Lower Yucca Formation boundary in Echo Canyon by Geophysics Master's Thesis student Myra Guerrero in March of 2017. With this acquired "birds-eye" view, I generated a distortion free 3D SfM model using Agisoft PhotoScan Professional software in conjunction with Maptek's I-Site Studio to develop a point cloud as well as a 3D mapping interface. This served as a mapping base during and after fieldwork to gain additional perspective on the study area tectonism and associated faults that I hypothesized had great influence on the RCFs lake cycle and subsequent formation (Figure 8).

5.1.3 Sampling Strategy

Four primary sites were selected for sample collection, the Squaw Canyon, the West Echo Canyon, and the East Echo Canyon sites, as well as the Bluff Mesa site. The former three localities belong to the same stratigraphic unit, the lower-most lacustrine cycle (Unit 2) of the Upper Yucca Formation, whereas the Bluff Mesa site belongs to the Bluff Mesa Formation, which overlies the Upper Yucca Formation. Below, two questions of this study are presented, followed by a brief introduction of key geologic differences between these sites, which constitute the rationale for the sampling approach.

1. *One or many lakes, one or many biogeochemical settings?* Septarian nodular concretions (SNCs) are abundant in each lacustrine cycle of the Upper Yucca Formation. Also within

the Bluff Mesa Formation, which was deposited after a marine transgression, nodule rich beds have been documented (Anderson, 2017). Despite being located in the same stratigraphic position as the Echo Canyon sites, which show evidence for syndepositional deformation, the Squaw Canyon site does not exhibit evidence of faulting caused by syndepositional extension. This raises the question if the SNCs from Squaw Canyon and Echo Canyon were formed in the same lakebeds or if they were exposed to different geochemical conditions than those from Echo Canyon.

Rationale for sampling nodular concretions from all for sampling sites: Comparison of SNCs from the lower-most lacustrine cycle from the three sites in the Upper Yucca Formation will reveal if there are fundamental geochemical differences between the sites, which could imply that the SNCs formed in physically separated water bodies. To obtain a relative assessment of the similarities/differences, the data set can be compared to the nodules from the Bluff Mesa Formation, which, thanks to the marine transgression, should have marked differences from the lakebeds found in the Upper Yucca Formation.

2. *A link between RFCs, syndepositional faults, and geochemical setting?* Radial carbonate fans are only found in the vicinity of Echo Canyon, and solely within Unit 2 of the Upper Yucca Formation, where abundant syndepositional faulting took place. At the East Echo Canyon site, I discovered a large number of RFCs during my January 2016 expedition. The correlation of this lakebed with the West Echo Canyon site required a revision of the structural interpretation by Li (2014a).

   Rationale for sampling RFCs from the East and West Echo Canyon sites: The uniqueness of the RFCs, and their relative proximity to syndepositional faults triggers the question if these features form in a unique geochemical setting that is controlled by fluids that enter

the lake along the fault plane. The comparison of the petrographic and geochemical signatures of the RFCs within a single sample (along and across growth rinds), between samples from the same site, and between sites, as well as the comparison to the observations from the SNCs can reveal if there was a special geochemical environment that permitted the formation of these features.

5.2 THIS SECTION PETROGRAPHY

Rationale for thin sections: Study if there are mineralogical differences between SNCs and RCFs, to identify what makes up the layering of RCFs' growth rings, to identify fossils in RCFs that are presumed to grow in water column. Moreover, considering the Upper Yucca Formation as a reservoir analogue to the South Atlantic Margin, with clay-rich lake beds as seals, the concretions and fans within those beds could be critical with regards to overall permeability of lake beds, and thus affect reservoir quality. Therefore, special attention was given to diagenetic features such as permeability and porosity.

Thin section analysis was performed on the samples collected from the East Echo Canyon site and the West Echo Canyon site. This type of petrographic analysis was used as a tool to identify carbonate types, dolomite or calcium carbonate, recognition of overprinting by fluid migration, and on the detritus, (i.e. siliciclastics, authigenic silicates, cement types and diagenetic features) to indicate primary and secondary pore water chemistry.

Hand specimens were slabbed and cut into billets (approximately 30x50x10 mm) with the use of Dr. Brunner's personal rock saw. The specimens were then sent out to Spectrum Petrographics in Vancouver, Canada for thin section creation, which included alizarin red and potassium ferricyanide staining to identify carbonate types. The alizarin red stain is used to distinguish between dolomite (which does not stain) and limestone (red stain), whereas the

potassium ferrocyanide staining is used to identify the presence of carbonate phases that contain ferrous (reduced, i.e. Fe^{2+}) iron (blue stain). Additional microscopic analyses focused on the identification of grains (i.e. siliciclastics, presence of fossils, peloids), grain size and abundance of grains, crystal fabrics, and on the detritus mineralogy aforementioned above.

5.3 GEOCHEMICAL ANALYSES

Rationale: There are multiple geochemical tools to address the questions if there is 'one or many lakes, one or many biogeochemical settings', and if there is 'a link between RFCs, syndepositional faults, and geochemical setting'. Originally, the proposed plan was to compare multiple geochemical fingerprints of samples obtained from: a) within syndepositional faults (vein fills), b) cements in lithologies adjacent to syndepositional faults, to c) the geochemical signatures of SNCs and RCFs. This comparison would have yielded insight into the question of fluids that migrate along the faults were the cause for the formation of SNCs and RCFs. Prime target for this approach would have been the isotope signature of cations that are associated with carbonates, such as calcium or strontium isotope signatures. During my field work it became apparent that it is exceedingly difficult to collect: a) representative vein fill samples from within the syndepositional faults and from b) cements in lithologies adjacent to syndepositional faults. There is plenty of vein material cross-cutting SNCs and RCFs, however, for a geochemical comparison this material is likely inadequate, because it was precipitated subsequent to the formation of the carbonate features.

Abandoning cation isotope signatures as geochemical proxy, I decided to focus my geochemical analyses on the carbon and oxygen isotope signatures of the carbonate and on the isotope signature of sulfate associated with the carbonate. In a nutshell, the carbon isotope signature of carbonates provides information on the carbon cycling in the aqueous environment in

which SNCs and RCFs formed, the oxygen isotope signature provides information on the water cycle within this environment, and the isotope composition of sulfate provides information on the presence or absence of reductive sulfur cycling, a biochemical process that often mediates carbonate precipitation. Without the direct link to the geochemical composition of the fluids that may have migrated along the syndepositional fluids, this suite of complimentary geochemical information holds the greatest potential to address key questions about the genesis of SNCs and RCFs in the Upper Yucca Formation.

5.3.1 Sulfate Extraction from Carbonate Samples

I attempted to extract carbonate associated sulfate (CAS) from all test sites, comprising SNCs from each site, and the RCFs of West Echo Canyon and East Echo Canyon. The CAS extraction follows an established sequential procedure, that has been refined – and adjusted to specific conditions – over the last decades by a number of research groups (e.g. Ziegenbalg et al., 2010; Wotte et al., 2012), including Dr. Brunner's research team (Montelongo, 2017; Bergersen, 2014; Gischler et al. 2017). In brief (see Figure 9), approximately 50 g to 70 g of clean (no weathering crusts) material is crushed with a hand mortar and sieved through a 150 micron USA Standard Test Sieve to ensure a consistent grain size. From this rock powder, easily soluble sulfate (ESS, such as gypsum or anhydrite) is removed by leaching with a sodium chloride solution (NaCl, 2 M) for no less than 24 hours with the use of test tube rotators. The samples were then placed into a centrifuge to be separated from the fluid (supernatant). The supernatant was transferred to a syringe fitted with a 0.45 µm membrane filter and filtered into a beaker. Subsequent to this step, the carbonate is dissolved with hydrochloric acid (HCl, approx. 6 M), which liberates CAS. The extracted ESS and CAS are collected via the addition of a barium chloride solution to the respective solution, which induces the precipitation of all sulfate as barium sulfate ($BaSO_4$). At all stages of

the extraction, sample weights are carefully recorded, such that ESS and CAS contents can be determined.

5.3.2 Carbon and Oxygen Isotope Analyses

Aliquots (~ 1g) of powdered samples were drilled with a Dremel tool and were taken for carbon and oxygen isotope analysis. A total of 80 samples were sent out to the light stable isotope facility at the Department of Geology, ETH Zurich, Switzerland. Of the samples that were sent to Zurich, a total of 48 aliquots corresponded to samples from two different RCFs, one from West Echo Canyon and one from East Echo Canyon. For each of these RCFs, a total of 24 individual samples. The purpose of this sampling approach was to obtain transects along and perpendicular (followed noticeable growth rims) to the apparent growth direction of the calcite crystals in the RCFs, which should reveal if there were changes in the geochemistry during the growth of individual RCFs. The remaining 32 samples focused on testing the matrices and the cements of the SNCs from each site, in order to establish if there are differences or similarities between the aqueous solutions from which the SNCs and RCFs formed.

The carbon and oxygen isotope composition of carbonates were reported according to the common standard delta notation:

$$\delta^{13}C_{sample}=(R^{13}C_{sample}/R^{13}C_{VPDB}-1)*1000‰$$

and

$$\delta^{18}O_{sample}=(R^{18}O_{sample}/R^{18}O_{VPDB}-1)*1000‰,$$

with $R^{13}C_{sample}$ corresponding to the isotope ratio $^{13}C/^{12}C$ of a sample, $R^{13}C_{VPDB}$ corresponding to the isotope ratio $^{13}C/^{12}C$ of Vienna Pee Dee Belemnite (VPDB, an international standard), $R^{18}O_{sample}$ corresponding to the isotope ratio $^{18}O/^{16}O$ of a sample and $R^{18}O_{VPDB}$ corresponding to the isotope ratio $^{18}O/^{16}O$ of VPDB.

6. RESULTS

6.1 FIELD OBSERVATIONS

6.1.1 Map & Digital 3D Model of Study Area

I established a new geological map of the study area (Figure 7), and with the help of photogrammetry a distortion free 3D model (Figure 8). The latter was used as a base for mapping as an additional perspective to the observations based on fieldwork, particular for the identification of faults.

6.1.2 Discovery of RCF at the East Echo Canyon Site

In 2014, Li discovered the radial carbonate fans in Echo Canyon and mapped their distribution to the northwest from Echo Canyon road (here referred to as West Echo Canyon site). Through extensive field work and assistance from UAS drone photogrammetry, I now established that, 1) in the study area, RCFs can only be found in the lowermost lacustrine cycle (Unit 2) of the Upper Yucca Formation and 2) RCFs in Unit 2 continue to the southeast of Echo Canyon road up to a distance of about 1 km. This lacustrine bed contains abundant and well-preserved RCF (Figure 7). The area within which the fans are found displays multiple faults, whereas there are fewer faults with much less offset in areas of where Unit 2 does not contain fans.

6.1.3 Measured Sections

To obtain a detailed documentation of the basal fluvial and lacustrine cycles Units 1-4 (Figure 7) of the Upper Yucca Formation three stratigraphic sections were measured within the southeastern area of Echo Canyon (Figure A1-A3). The sections are approximately 250 m apart spanning a distance of 500 m (Figure 7). The southeastern area of Echo Canyon has a more

complex structural makeup than the area west of Echo Canyon, and comprises considerable relief of up to 100m. Despite these challenges, it was possible to: 1) stratigraphically correlate the fluvial and lacustrine cycles and 2) to determine the amount of offset associated with faults.

Unit 1 is 20-22 m thick and is dominated by a coarser grained sandstone facies than observed in overlying units of the Upper Yucca (Fox, 2016) and varies in fresh surface color from pink to gray to buff. The sandstones are interbedded with sub rounded to sub angular clasts of pink, white and black chert, quartz and limestones. The base of unit 1 can be identified by a sharp fining upward contact and color change observed within the conglomeratic dominated sandstones of the Lower Yucca from dark red to light red-pink (Figure 10).

Unit 2 is 6-7 m thick and is identified as a shaly lacustrine facies, which is host to the RCFs in Echo Canyon, but also is composed of SNCs, irregular carbonate nodules, and dense mudstones. From the basal portion of Unit 2, the lacustrine cycle fines upward from mudstones to the clay rich bed of which the RCFs and SNCs outcrop. In measured section one, a conglomeratic fluvial channel caps unit 2 (Figure 11), whereas in the other two measured sections it is capped by gray medium-grained sandstone. This bed makes up a small amount of the stratigraphic column and, due to the abrupt transition into the sandstones of Unit 3, is interpreted to have been deposited in shallow water.

Unit 3 is the 2nd sandstone cycle of the Upper Yucca, and is bounded by lacustrine mudstones of Unit 2 and Unit 4. This unit has a drastic change in thickness as it ranges from 65m proximal to Echo Canyon road to 26m above fan alley (Figure 7). This is interesting because it accounts for the approximate 40 m offset that is observed with this wedge at Echo Canyon road and from “Fan Alley” that is located approximately 350m SE of Echo Canyon Road.

Unit 4 is 12-14m thick and is the 2nd lacustrine cycle of the Upper Yucca Formation. This bed is observed to have a stromatolitic bindstone lithofacies (<50 cm thick) that is approximately 10m from the base and overlies the massive mudstone and fissile shale bed containing SNCs (Figure 12). The lateral correlation of these stromatolites extends 600m to the SE from Echo Canyon road (Figure 7). This facies is easy to identify as it has stark yellow-orange gray color that contrasts with rusty weathering patches as opposed to the reddish bed of SNCs. From this measurement it is not clear if the stromatolitic bed is continuous throughout however Li 2014 documents that west of Echo Canyon the lateral extent of these features ranges up to 50m.

The measured sections brought to light the amount of offset that is associated with a major fault in East Echo Canyon site. Several small-scale faults (1 – 5 m) are observed in Echo Canyon however a major graben block, here now referred to as "the wedge" has a measureable offset of 40 m. This fault is directly adjacent to Echo Canyon Road and to "Fan Alley".

6.2 PETROGRAPHIC ANALYSES

6.2.1 Outcrop Study / Hand Samples

The Upper Yucca lacustrine cycles are composed of primarily reddish mudstones that are interbedded with shales. These sediments are host to SNCs that are present in every cycle and RCFs of Unit 2 only found in the vicinity of Echo Canyon. Outcrop of this facies is commonly characterized by friable, reddish to light brown sandstone that is less resistant to weathering.

The SNCs vary significantly with regards to their geometry, size, and color in the study area. Despite having an array of colors and shades from bright red, orange, yellow, green, gray, they all weather out of reddish fine-grained sediments and appear on the surface as float (Figure 13). These concretions can range in sizes from a few centimeters to coalescing into large

irregular bodies, even sometimes appearing columnar, that can measure up to a meter tall. It is observed that in the process of their growth and formation, they are cemented together and remain in situ with no pattern relative to the bedding.

Individual samples were cut and inspected with a hand lens. All nodules contain some degree of septarian cracks but it is evident that some are better developed than others ranging in widths of 0.25 cm to 5 cm. Cracks are often connected and coalesce with each other forming larger cracks. The majority of Septarian cracks are white calcite but some display dark gray coloring surrounding the rims (Figure 13). There are also crosscutting dissolution veins (less than 0.05 mm) that indicate that veins that formed after the septarian cracks began generation. For nodules that are found in Unit 2 and are associated with RCFs, there is a sharp contact between the matrix of the nodule and the fan in the transition zone.

Carbonate fans

RCFs only crop out in unit 2 near Echo Canyon. The purple spherical or elliptical features are very dense and are resistant to weathering and vary in size from 1 cm to 0.5 m. Calcite crystals range in in length from 0.1 mm to 2 mm and in width from 0.05 mm to 0.15 mm. The crystals of RCFs stack and radiate outward in a spherical orientation. In some samples, multiple generations or defined layers combine to form a thicker fan. Layering in the fans is not present in all samples but when present it is appears to be rhythmic, having similar sized bands, before calcite crystals become massive. Clay seams define the contacts of each layer and crystals of the fan are truncated by this contact, however generation of fan crystals grows on the subsequent layer. Unusual patches ranging in color from green, gray, white and orange exist within the matrix of the RCFs that follow the “vertical” orientation (Figure 14).

6.2.2 Thin Sections

Thin section analysis was conducted on 16 samples from West Echo Canyon site and East Echo Canyon site. Thin sections were examined to aid in the interpretation of primary carbonate mineralogy and diagenesis as well as insight to any, if applicable, geochemical variations in the carbon or oxygen isotope composition of the carbonate.

All of the examined samples are cemented with a combination of calcite phases that range from micrite to bladed to equant course grained. Septarian fractures are often filled with mega coarse calcite crystals but can have finer grained equant or bladed crystals surrounding the rim (Figure 15). Abundance of detrital quartz grains vary with sample but are generally observed to be "floating" in the matrix (Figure 15). Fossils are non-existent.

The majority of these thin sections indicate oxidized iron oxides (brown stained) however it is observed that 2 samples that were retrieved from the major fault near fan alley had ferroan (iron rich) baroque dolomite (Figure 15). Dolomite is observed in very small amounts within four samples of Unit 2, EEF1, EEFN3-2, EEF4, EEF5-2 (Figure 15), however dolomite is abundant in one sample from Unit 4 (Figure 15), which had been identified as a dolomudstone by Li (2014). With regards to lacustrine sediments in the Upper Yucca, dolomite is predominately a replacement product that can indicate a hypersaline sabkha environment or is a result of hydrothermal fluid exchange that infiltrated into a porous body. Very little primary porosity within the RCFs and SCNs exist as they are composed of mudstone and would be difficult to exchange fluids. However, the presence of ferroan baroque dolomite in two samples from the fault zone indicates that this area was exposed to hydrothermal and possibly high temperature fluids.

In summary, the carbonate concretions and fans entrap and preserve minerals with a sedimentary and authigenic/diagenetic origin.

6.3 GEOCHEMICAL ANALYSES

6.3.1 Sulfate Content of Samples

Despite employing a method for the extraction of ultra-low sulfate contents that was developed by Masters student Marisela Montelongo (Montelongo 2017), no measurable quantities of ESS or CAS could be extracted. Consequently, no sulfur or oxygen isotope analyses of ESS or CAS could be carried out.

6.3.2 Carbon & Oxygen Isotope Composition of Carbonates

Stable oxygen and carbon isotope values obtained for the powders extracted from all four sites are presented. Both oxygen and carbon isotope data show negative values and reveal little differences. The range of $\delta^{18}O$ values is (-13.11 to -3.71‰) with a mean value of -6.60‰. The range of $\delta^{13}C$ values is (-14.64 to -4.62‰) with a mean carbon isotope value of -7.33‰.

7. DISCUSSION

7.1 LAKE BEDS IN THE UPPER YUCCA FORMATION

This work builds on two Master's thesis projects that were carried out shortly before (Li, 2014) and in parallel to this study (Fox, 2016). Here, a brief overview of the findings of these projects is given, with focus on observations that are central to this study. The Upper Yucca Formation in the Indio Mountains consists of alternating units of sandstone and shale. The shale units within the Upper Yucca Formation were interpreted by Li (2014) as lacustrine deposits that are capped by fluvial strata. Li (2014) identified 11 upward-shallowing fluvial-to-lacustrine cycles. Fox (2016) re-correlated marker beds of the Upper Yucca Formation strata from Echo Canyon to Squaw Canyon and found that some of the units identified by Page (2011) and Li (2014) had been previously miscorrelated. These findings resulted in a reduced number of 10 cycles, which build the stratigraphic framework for this study (Figure 16). Li (2014) documented RCFs and SCNs in the lake beds, however, the geologic history of the RCFs, and their distribution in the lake beds, remained unresolved.

7.2 IMPLICATIONS FOR THE INTERPRETATION OF KINEMATICS OF FAULTS FROM THE FINDING OF RCFS

The primary focus of this study was to document and understand the relationships between radial carbonate fans (RCFs) and nodular concretions (SNCs), such as where they are found in outcrop, their geometry (e.g. if nodules are required as substrates for fans to grow), or if there is a systematic geochemical relationship between these diagenetic features. Through extensive fieldwork, and assistance from UAS drone photogrammetry, I established that in the study area, RCFs can only be found in the lowermost lacustrine cycle (Unit 2) of the Upper Yucca Formation. In January 2016 I found the continuation of Unit 2 to the southeast of Echo Canyon road up to a

distance of about 1 km. This lacustrine bed contains abundant and well-preserved RCFs (insert figure of Echo Canyon). This finding required that the previous interpretation of the structural relationships between faults intersecting in Echo Canyon (Li, 2014) needed to be revised. In essence, what has been previously interpreted as down dropped graben blocks (Li, 2014; Figure 17) is now interpreted as one major syndepositional fault (Figure 7) that was actively moving during the deposition of lakebed 1 (Unit 2) and Unit 3. This syndepositional fault is geographically at the center of the area where the FCFs are found (Figure 18). It appears that this geographic relationship is not coincidental, because it coincides with the distribution and size of the RCFs. Nearest to the fault, the RCFs are abundant and can be found every 2 m and largest (up to 0.5m in size). Moving away from the syndepositional fault, the abundance diminishes and the fan size becomes smaller, until only fan fragments are found (Figure 18). A consequence of this re-interpretation is that the RCFs are not restricted to settings within grabens, but may still be located in a setting that allows for a causal relationship between the syndepositional faulting located at Echo Canyon and RCF formation.

7.3 Estimate of Offsets on Faults Based on Mapping, Digital 3D Model, and Measured Sections, and Assessment of Syndeposition

A combination of tools was used to determine the stratigraphic correlation on the basal units of the Upper Yucca in the East Echo Canyon site and their relationship to the corresponding beds that lie NNW of this study area from Echo Canyon road. From my observations, I was able to deduce the amount of offset associated with faults in this area. Two faulted boundaries that are located in the West Echo Canyon site have similar offsets of 5 m (Figure 7) and in the East Echo Canyon site offsets of 2 m and 7 m. These are small in comparison to the roughly 40 m offset of the ‘Wedge’ (Figure 7). The Wedge is a graben block that lies between Fan Alley and Echo

Canyon Road. With the aid of a measured section taken from the Wedge, it is evident that the fans belong (unit 2 of the Upper Yucca) to a continuous lakebed (Figure 18), however the thickness of unit 2 in this graben block is approximately 7.5 m with an additional meter of covered float. This represents a thickness change of minimally 1.5 m from the other two measured sections. The actual thickness of the lake bed in the wedge could actually be larger, because the top of the outcrop is covered. This finding is clear evidence that this fault was syndepositional, i.e. it was moving during the deposition of the lowermost lake sediments. In the Wedge, a fluvial conglomerate that measures 3.5 m in thickness and contains large rip up clasts of nodules and fan fragments, caps Unit 2. In contrast, the other two measured sections show that Unit 2 is 5.5 m to 6 m thick and is capped by 2 m of medium-grained sandstone, followed by 0.7 m of a fluvial conglomerate. This can be interpreted as a paleo-high, which indicates that they were deposited on a horst block. The Wedge represents a graben that was filled with clastic sediments as this block continued to drop. Consequently, Unit 3 in the wedge measures a total of 65 m whereas it measures 26 m above 'Fan Alley'. From this observation follows that the syndepositional fault remained active during the deposition of Unit 3. Unit 3 is capped by this continuous lakebed (Unit 4) that displays no faulting or spatial disruption over the measured area (a distance of 600 m from Echo Canyon Road) and measures 12-14 m. Thus, at the time of the deposition of the second lake bed (Unit 4), movement at the syndepositional fault had ceased.

7.4 ISOTOPE CHEMISTRY OF RCF & SNC

Collectively, all samples from the Upper Yucca Formation have light $\delta^{13}C$ and $\delta^{18}O$ values (Figure 19). The range of $\delta^{13}C$ values is (-14.64‰ to -4.62‰) with a mean carbon isotope value of -7.36‰ and the range of $\delta^{18}O$ values is (-13.11‰ to -3.71‰) with a mean oxygen isotope value of -6.55‰. The nodule samples from the Bluff Mesa Formation show ranges of $\delta^{13}C$ from (-

8.21‰ to -4.62‰) with an average carbon value of -5.89‰ and $\delta^{18}O$ ranges from (-8.54‰ to -5.33‰) with an average value of -6.17‰. This shows that the samples of the Bluff Mesa Formation are slightly enriched in ^{13}C compared to the samples from the Upper Yucca Formation, whereas the $\delta^{18}O$ values overlap, with values that are indicative for a freshwater body ($\delta^{18}O$ values for marine carbonates typically show slightly positive values; Clayton and Degens, 1959; Talbot and Kelts, 1990). This finding could indicate that the samples from the Bluff Mesa Formation have been formed in water that contained carbonate that was less depleted in ^{13}C, either because of an influence from marine water on a freshwater body (e.g. a brackish lake) or different carbon isotope composition of carbonate dissolved in meteoric water.

The lightest value of -14.64‰ for $\delta^{13}C$ belongs to the cement of one SNC (sample L5AC), which was obtained from the uppermost lake cycle of the Upper Yucca Formation. Other cements range from (-8.51‰ to -6.49‰ $\delta^{13}C$) and do not show such a strong depletion in ^{13}C. Because the cements in septarian nodules represent a later precipitate (Astin 1986), these values are not considered in the subsequent discussion of the lake chemistry. The heaviest recorded carbon isotope composition (-5.72‰) was from the matrix of a SNC from the first lake cycle of the Upper Yucca Formation, but was located near the main fault adjacent to Fan Alley (Figure 18) the dextral portion of the Wedge. The sample shows a light orange color, and its oxygen isotope composition is -13.11‰, which is strongly depleted in ^{18}O relative to all other samples. This indicates that fluid flow along the fault had a major impact on the oxygen isotope signature, and possibly also on the carbon isotope composition of the sample.

The range of the carbon isotope composition of RCF and SNC matrixes overlap, whereas the oxygen isotope composition of the SNC matrixes tends to be lighter than the oxygen isotope

composition of the corresponding RCF. The average oxygen isotope composition of the East RCF (-6.89‰) is lighter than the isotope composition of the West RCF (-5.84‰).

Zooming in on an individual fan, different patterns are observed for the oxygen and carbon isotope composition. Comparing three bands with higher accumulation of clay minerals, we see relatively light oxygen isotope compositions for the outer (samples 25-29) and innermost bands (samples 9-16), with the center band having heavier oxygen isotope compositions (samples 1-8; Figure 20). Within a band that has little clay, the isotope values are consistently light (Fig 21 – blue colored dots labeled A-J). The carbon isotope composition for the outermost band is lightest, followed by the central band, and the innermost band, a pattern that is also observed for the band with little clay (Figure 21). A cross-plot of the carbon and oxygen isotope composition of the samples within the band with little clay reveals a potential positive correlation, i.e. heavier carbon isotope values coincide with heavier oxygen isotope compositions. In the following, these observations are discussed in the geological and palaeo-geographical context of the Upper Yucca Formation.

7.5 CARBON & OXYGEN ISOTOPE COMPOSITION OF LAKE CARBONATES

Stable isotopes of lake sediments are often used as proxy to reconstruct paleoclimates (Talbot and Kelts, 1990; Leng and Marshall, 2004). A persistent problem in the quantitative interpretation of data is that the studied systems are inherently unique; therefore, variables in isotopic compositions are influenced by a wide range of interlinked environmental and geological processes and not controlled by a single factor (Leng and Marshall, 2004). In lacustrine environments, stratigraphic changes in $\delta^{18}O$ values are commonly attributed to changes in temperature or precipitation/evaporation ratio; whereas changes in $\delta^{13}C$ values indicate changes –

that may be controlled by changes in climate – in nutrient cycling and productivity within the lake and its catchment (Leng and Marshall, 2004).

7.5.1 Oxygen Isotope Composition of Lake Carbonates

The $\delta^{18}O$ values of lake carbonates are a function of lake water composition and mineral precipitation temperature (Talbot and Kelts, 1990). The lake water oxygen isotope composition depends mainly on: (1) the isotopic composition of the rainwater in the hydrographic basin area, (2) the availability and seasonality of the rainwater, (3) temperature, (4) evaporation rate, and (5) relative humidity (Alessandretti et al. 2015). Rain water is isotopically light, with precipitation from higher altitudes (i.e. snow) typically being lighter than rain water from lower altitude (Leng and Marshall, 2004). The water temperature not only affects evaporation rates, but also the oxygen isotope fractionation between dissolved carbonate and precipitated carbonates: lower temperatures result in a larger enrichment of precipitated carbonates in ^{18}O relative to carbonate in solution, which can be summarized as 'the colder, the heavier'. Temperature, relative humidity, and evaporation rates are intimately linked, and play an important role in the balance between input of water into a lake system via rivers or groundwater discharge that typically supplies isotopically light water (Leng and Marshall, 2004), and the evaporation that removes isotopically light water (Hoefs 2008; Figure 22). If this balance tips toward strong evaporation, positive $\delta^{18}O$ values are expected, a situation that is typical for lakes that have no outflow, referred to as 'closed lakes', whereas in 'open lakes' that have large input and outflow of water thanks to precipitation, negative $\delta^{18}O$ values are expected to be observed (Figure 19). Closed lakes, are expected to show much stronger fluctuations in their water balance, which leads to the expectation that carbonates from such lakes should exhibit a wider range in $\delta^{18}O$ values than open lakes, which is indeed observed (Figure 19).

7.5.2 Carbon Isotope Composition of Lake Carbonates

The interpretation of $\delta^{13}C$ in lacustrine systems is more intricate than its $\delta^{18}O$ counterpart because there are more drivers that influence the system (Figure 23). The major parameters responsible for carbon isotope fractionation in lacustrine and marine environments are (for a review, see Alessandretti et al., 2015): (1) primary productivity in the surface water, which preferentially removes ^{12}C from the environment and results in positive $\delta^{13}C$ values for carbonate and causes organic matter to be isotopically light; (2) temperature-dependent carbon isotope fractionation between dissolved and precipitated carbonate fluctuations, which in analogy to the oxygen isotope fractionation follows the rule of thumb 'the colder, the heavier'; (3) oxidation due to biological degradation of isotopically light organic matter, which returns ^{12}C to the water column and thereby induces lighter $\delta^{13}C$ values for dissolved carbonate; (4) methanogenesis (a form of fermentation of organic matter) that produces methane that is strongly depleted in ^{13}C and carbonate that is enriched in ^{13}C; (5) subsequent oxidation of methane to carbonate, which results in light $\delta^{13}C$; and (6) carbon isotope exchange between dissolved carbonate in surface water and atmospheric carbon dioxide (CO_2), which produces carbonate that is enriched in ^{13}C relative to CO_2 by approximately 9‰ (i.e. +2.5‰ for a $\delta^{13}C$ of CO_2 to -7.5‰, which is typical for today, but may have been heavier in the Early Cretaceous) (Armstrong and Brasier, 2005; Alessandretti et al., 2015). Additional factors that contribute to $\delta^{13}C$ signatures in lake sediments are water recirculation and mixing in otherwise stratified lakes, which brings ^{13}C-depleted carbonate (light due to oxidation of organic matter) to the surface; micro-habitat effects related to variations in metabolic processes of many different species associated with carbonate precipitation (e.g. C4 and C3 plants); and diagenetic processes in which interstitial fluids tend to preferentially capture ^{12}C, resulting in slightly negative values (Armstrong and Brasier, 2005; Alessandretti et al., 2015).

These various processes probably similarly affect the range of $\delta^{13}C$ values for carbonates from open and closed lakes, and the observed range of $\delta^{13}C$ values may be more representative for the different locations in a lake system where carbonates form (deeply buried in the sediment: heavy isotope composition due to carbonate from methanogenesis; in sediment or at sediment-water interface: light because of oxidation of organic matter and methane; in surface water: heavy due to photosynthesis and CO_2 exchange between water and air; Leng and Marshall, 2004).

7.5.3 Oxygen & Carbon Isotope Composition of Lake Carbonates

In closed lake systems, a positive correlation between $\delta^{13}C$ and $\delta^{18}O$ can sometimes be observed (Figure 24). Typically, this correlation is attributed to a link between enhanced evaporation (driving the $\delta^{18}O$ of water heavy) and a shift in the balance of photosynthesis relative to CO_2 exchange between the lake water and air towards a higher impact of photosynthesis. Curiously, the nature of the link between the evaporation and the shift in the balance in carbon cycling in favor of photosynthesis is not well discussed in the literature. It can be speculated that increased salinity caused by evaporation leads to a decrease in the exchange of CO_2 air and water. Photosynthesis removes isotopically light carbon, driving the $\delta^{13}C$ of carbonate heavy, whereas CO_2 exchange between the lake water and air drives the isotope composition of carbonate to a constant heavy isotope signature of 2.5‰. In lakes that have relatively heavy $\delta^{13}C$, this relationship would lead to a positive correlation between $\delta^{13}C$ and $\delta^{18}O$. However, in lakes that exhibit negative $\delta^{13}C$, both CO_2 exchange between the lake water and air and photosynthesis drive the carbon isotope composition heavy, thus the inferred link between enhanced evaporation and diminished CO_2 exchange would not necessarily yield a positive relationship between $\delta^{13}C$ and $\delta^{18}O$ of carbonates.

7.6 IMPLICATIONS FOR CLIMATE DURING UPPER YUCCA TIME FROM LAKE CHEMISTRY

The carbon and oxygen isotope composition of the SNC matrixes and RCF can be considered signatures that are related to the lake chemistry. The comparison to trends of open lakes and closed lakes systems (Talbot and Kelts, 1990) is intriguing (Figure 24). With their light carbon and oxygen isotope signatures the data for the Upper Yucca lake samples plot in the quadrant of lakes that persistently gain and lose water through rivers, i.e. open lakes. The relatively light oxygen isotope signature of the carbonates indicates dominance of freshwater input, which is in good agreement with the finding that the content of CAS of SNCs and RCFs was very low, indicating that sulfate was almost absent from the studied lakes. Interestingly, the spread in the oxygen isotope composition for the Upper Yucca lakes (~5‰ for $\delta^{18}O$) is much larger than the spread for carbon isotope compositions (~2.8‰ for $\delta^{13}C$), a pattern that is not observed for the open lakes (Talbot and Kelts, 1990), which display larger carbon isotope than oxygen isotope variation (~5‰ for $\delta^{13}C$ vs. ~3‰ for $\delta^{18}O$). The large spread for $\delta^{18}O$ is more typical for closed system lakes, i.e. lakes with no outflow (Talbot and Kelts, 1990). Closed lakes often display a correlation between $\delta^{18}O$ and $\delta^{13}C$, a pattern that is not observed for the Upper Yucca samples. This indicates that the lakes from the Upper Yucca Formation may display attributes from open and closed system lakes, i.e. strong fluctuations in the relationship between evaporation and freshwater input while maintaining some level of in- and outflow. A potential scenario would be lakes that are intermittently supplied with river water, while receiving considerable water from groundwater discharge. Considering the permeability of the fluvial deposits in the Upper Yucca Formation this appears to be a valid option. The presumably warm climate during the Early Cretaceous at elevated temperatures due to the paleogeographical location are expected to have minimized fluctuations in $\delta^{18}O$ of carbonates due to isotope fractionation during carbonate

precipitation (diminished equilibrium isotope fractionation at elevated temperatures, for a review, see Hoefs, 2008), but would have allowed for a large range of $\delta^{18}O$ due to high and variable evaporation rates, however it is unclear if the lakes were alkaline. The absence of fossils implies the conditions may not have been hospitable for animal life. At least one lake bed (Unit 4, Lake cycle 2) that has stromatolites. The presence of these features indicates that within this lake cycle, the lake flourished with microbial activity that include algae, bacteria, fungi and protozoans that had a sufficient amount of calcium carbonate to form (Burne and Moore, 1987; Riding 2000, 2006; Li, 2014) and thrived in an oxygenated environment in shallow waters where photosynthesis occurs (Riding, 2000). No stromatolites were documented in the 1st lake cycle where the RCFs formed.

7.7 Implications for Lake Hydrology from the Oxygen Isotope Relationship Between RCF & SNC

Taking a closer look at the $\delta^{18}O$ of SNC and RCF samples (Figure 25), the SNCs tend to be isotopically lighter in than the RCF samples. This separation indicates that the SNCs were formed in waters that were more depleted in $\delta^{18}O$ than the waters in which the RCFs were precipitated, or that the water from which the RCFs precipitated, were colder than the water in which the SNCs formed. From the petrographic observations it is evident that the septarian concretions were formed first, and then at a later time the fans accreted onto the septarians. An interesting factor to consider is that the SNCs were formed in the sediment, below the sediment-water interface. This raises the question if the sediments in which the SNCs formed in were in contact with a large groundwater body (lighter $\delta^{18}O$) associated with the highly permeable fluvial sediments that are cyclically deposited throughout the Upper Yucca Formation, while the fans

formed in the water body that was slightly more enriched with $\delta^{18}O$ due to strong evaporation of the lake water.

7.8 LAKE BED 1 – RCFS AS A UNIQUE ARCHIVE OF LAKE CHEMISTRY

While SCNs are present in every lake cycle of the Upper Yucca, RCFs are not. The lake body from which the RCFs were precipitated in must have had some very unique characteristics. In every case of outcropping *in situ* fans, it is observed that they have a nucleus represented by a SCN from which follows that the septarian nodules were already formed within the sediment before the fans could accrete and further develop. No truncation of the SCNs was found, which indicates that the SCNs were not subaerially exposed, i.e. not affected by erosion, prior to the growth of the RCFs. This finding supports the hypothesis that SCNs and RCFs were formed in the same lake. The West Echo Canyon RCF clearly display clay seams, but no indication for larger silt grains. The sole presence of clays, and absence of silt indicates that the seams are not related to storm events, that would have transported dust into the lake. Rather, the clay seams are likely condensed accumulations during times when the RCFs showed little growth, whereas clay-poor bands reflect times with comparably rapid growth of the calcite crystals.

Taking a closer look at the $\delta^{18}O$ signatures of sample WEFN (West Echo Canyon Fan) it becomes evident that the crystal matrix that lies in between the clay seam layers is the lightest with values ranging -5.8‰ to -6.1‰ (Figure 20, samples A-J). Of the three clay seams that were measured, the middle seam is the heaviest with $\delta^{18}O$ values ranging from -4.6 to -5.0‰ (Figure 20, samples 1-8), whereas the other two seams display values between -5.3‰ and -6.4‰. With the values between the clay bands oscillating from light to heavy to light, it is evident that there is no secular trend for the $\delta^{18}O$ of lake water during the formation of the RCF. Heavier $\delta^{18}O$ values could be indicative of times in which the balance between freshwater input and evaporation was

tipped toward increase evaporation, which would imply that the fans grew more rapidly during wetter times. Alternatively, it is possible that higher temperatures caused a smaller isotope fractionation between precipitated carbonate and water, with the temperature effect exceeding the enrichment in ^{18}O of water due to evaporation. This interpretation is appealing, because enhanced evaporation is expected to increase lake alkalinity (Al-Droubi et al., 1980), thereby accelerating fan precipitation.

Unlike the $\delta^{18}O$ signatures of sample WEFN, there is a distinct trend to lighter $\delta^{13}C$ from the innermost clay seam to the outside of the fan (Figure 21). The intriguing secular trend in $\delta^{13}C$ to lower carbon isotope compositions indicates that over time, the contribution of light carbon from oxidation or organic matter or methane increased. As the lake is essentially sulfate-free, and the SNC are embedded in clays that due to their low permeability prevent deep penetration of oxygen into the sediment it is evident that degradation of organic matter likely operated via methanogenesis. The produced methane likely formed bubbles that in some locations reached the aerobic sediment-water interface where it was oxidized, forming isotopically light carbonate ions, which contributed to the growth of RCFs. Because methane only becomes oxidized at the sediment-water interface where it gets in contact with oxygen, the flux of methane increases over time as organic matter bearing sediment accumulates (Figure 26). I speculate that these increased methane fluxes, associated with increased sediment thickness may be the driver of this secular change to lighter $\delta^{13}C$ values.

Finally, zooming in once more on the highest resolution, namely the band with low clay content, which may correspond to a time of rapid growth, I observe a positive correlation between $\delta^{13}C$ and $\delta^{18}O$ (Figure 21). The range of the observed $\delta^{13}C$ and $\delta^{18}O$ is small, and superimposed on the general trend to lighter $\delta^{13}C$ values towards the outside of the fans. It is unlikely that this

trend can be attributed to the positive correlation between $\delta^{13}C$ and $\delta^{18}O$ observed for closed lake systems, because the $\delta^{13}C$ values of the carbonates in the Upper Yucca Formation are isotopically light. Here, I propose three scenarios that may explain the positive correlation between $\delta^{13}C$ and $\delta^{18}O$ in the band that shows little clay content. First, an increase in insulation could have driven enhanced evaporation (heavier $\delta^{18}O$ of water) and enhanced primary productivity, which would drive the lake to more alkaline conditions (facilitates carbonate precipitation) and remove ^{12}C by incorporation into biomass causing the enrichment of carbonate in ^{13}C. Second, diminishing riverine input leads the a relatively enhanced recharge of lake water from groundwater. This would contribute isotopically lighter water, because it is not affected by evaporation, and groundwater infiltrating in a higher altitude may have lighter oxygen isotope composition. The groundwater is expected to also contribute isotopically light carbonate (Leng and Marshall, 2004) from the oxidation of organic matter in the aquifer, such as plant material. Presence of plant material in the fluvial sediments of the Upper Yucca Formation is evident from petrified wood that is found sporadically in float across the study area. As the groundwater carries dissolved calcium and carbonate, the precipitation of calcite is favored once the waters are discharged into the lake. Third, and in a variation to the second scenario, relatively enhanced contributions from fluids discharged from syndepositional faults could also account for the observed pattern. As these fluids are fed by groundwater infiltration, they are likely to cause a similar isotope relationship. This third option ties the observation of abundant RCFs in proximity to the faults with a geochemical sound explanation for the positive relationship between $\delta^{13}C$ and $\delta^{18}O$ in the band that shows little clay content.

7.9 LAKE BEDS IN THE UPPER YUCCA FORMATION – INSIGHTS FOR HYDROCARBON EXPLORATION

It is difficult to find a modern analogue that displays similar geochemical characteristics and geographically lies in the same tectonic and climate setting as the lacustrine/mixed siliciclastic presalt hydrocarbon reservoir deposits in the South Atlantic Margin (SAM). The Upper Yucca Formation, with its well exposed outcrops in the Indio Mountains is likely to be such an analogue, however, in itself it turns out to be a challenge to demonstrate that this is indeed the case, as limited data are reported in the literature, and key information regarding these petroleum systems is proprietary. Here, I make an attempt to assess the information gained from the lakebeds in the Upper Yucca Formation in the context of hydrocarbon exploration in the SAM.

Today, and despite the challenges by limited data sets, there is a growing number of literary works that provide general insight into evolution of the SAM basins. During the continental rifting phase of the SAM, twelve basins were developed along the eastern Brazilian margin (Bruhn et al., 2003). In a study recently published in 2016 (Dickson et al., 2016), it was reported that multiple lacustrine-sourced oils were encountered in various hydrocarbon plays around the South Atlantic, including NE Brazil, however, it is evident that a majority of the source rocks are marine, for example there is no indication for lacustrine source rocks offshore Ivory Coast and Ghana (Dickson et al., 2016). The predominant source rocks are marine sediments of Cretaceous age (Cenomanian–Turonian and possibly Albian). Likely, the asymmetry of the opening of the South Atlantic, which is today encountered as petroleum systems asymmetry across the South Atlantic Equatorial Margins, biased the location of lacustrine source rocks (Early to mid-Cretaceous pre-rift to early synrift) to the NE Brazil margin, notably the Campos Basin and Santos Basin. The lacustrine carbonates form the Santos Basin belonging to the Barra Velha Formation, which were

described by Terra et al. (2010) differ significantly from those illustrated from other basins and likely represent abiotic precipitates instead of microbialites (Wright and Barnett, 2015). Curiously, the observed carbonate features of the Barra Velha Formation show a strong resemblance with respect to the observed shapes of the carbonate features of the Upper Yucca lacustrine sediments. Spherulites and shrub textures have been reported, with shrubs sometimes growing on top of the spherulites – a pattern that looks conspicuously similar to the geometric relationship observed between RCFs and SCNs (Figure 27). However, it must be noted that the shrubs and spherulites have much smaller sizes than RCFs and SCNs. The conditions under which the shrubs and spherulites formed are considered to be sulfate-free hyper-alkaline shallow lakes (Tosca and Wright, 2016), a finding that coincides with the setting in which the carbonates from the Upper Yucca lakes formed. The Barra Velha Formation is an important reservoir rock (Petersohn et al. 2013), owed to large porosity created by the shrubs (Wright and Barnett, 2015; Tosca and Wright, 2015). With respect to the information gained from the lake beds in the Upper Yucca Formation in the context of hydrocarbon exploration in the SAM, it becomes clear that if the lake beds are to be used as analogue, one is looking at a reservoir, and not a source analogue. The relatively low abundance and location of the RCFs embedded in a clay-rich lacustrine sediment makes it evident that the lacustrine beds from the Upper Yucca Formation would make for a poor reservoir. Rather, they would make excellent seals, and could potentially cause compartmentalization of the fluvial sediments, which thanks to their porosity and permeability make for excellent reservoirs. Due to the small thickness of the lake sediments, it is likely that they would escape detection by seismic methods. A critical question that comes up is the lateral extension of these presumably shallow lakes. The fact that we find only clay sized particles in the RCFs points to a very distal source of the detrital material, which would indicate that the lakes must have been very large.

7.10 ADDITIONAL INSIGHTS - PHOTOGRAMMETRY

Recently, high-resolution three-dimensional (3D) mapping has become popular due to a growing demand to digitize data and present stronger visualizations on all scales in the geosciences from a single hand specimen to landscapes (McCaffrey et al., 2005, Bemis et al., 2014). In particular, high-resolution digital 3D data collection is dominated by active source sensors, predominantly based upon laser scanning technologies (e.g., LiDAR), which measure distance to a target based upon the travel time of reflected light (e.g., Hodgetts, 2013, Bemis et al., 2014). However, the most recent and widely accessible development, due to the rapid advancement of modern technology, allows for simple digital photography (i.e. digital camera) to collect high-resolution 3D data. The raw data is comprised of digital photographs, which can be collected with any commonly available digital camera, including those on smartphones and tablets (or a GoPro as is the case with this study), and facilitates rapid collection of large amounts of data in remote settings where portability and efficiency may be critical (Bemis et al., 2014). Photo-based 3D reconstruction techniques can provide a comparable resolution to laser scanning tools with a significant reduction in cost, infrastructure, and processing requirements (Bemis et al., 2014). In utilizing digital photography and coupling this with UAS (unmanned aerial systems), any geoscientist can easily visualize earth surface and topographic data in areas of interest. Additionally, once having this data digitized, it can be interpreted with proper software (e.g. Maptek's I-Site Studio) to create lifelike 3D models that have resolutions on the order of 1-2 meters (the resolution which I was able to obtain) that highlight key geologic features. 3D photogrammetric models and their accompanying digital photographs are inherently archival, easily shared and provide a record that is faithful to the primary observations, thereby allowing

future generations of geoscientists to extract additional 3D and oriented data, or reinterpret the outcrop/samples (Bemis et al., 2014).

3D photogrammetry with the aid of a drone, has emerged as a useful tool within the Indio Mountains, and has gained interest from works of other Master's Thesis students (Anderson, 2017) (Guerrero, unpublished). 3D mapping of this remote landscape can be utilized for those who are physically incapable of or inexperienced performing field geology in areas that have complicated structures or that have steep terrains (Pavlis and Mason, 2017), specifically areas of interest that have local relief of 200-300 m (e.g. Anderson, 2017). I was fortunate to have this technology available coupled with adequate software to aid my interpretation of the kinematic evolution of Upper Yucca lake cycle 1 where the only known locality of the RCFs exists (Figure 8).

8. CONCLUSIONS

The rifting events that created the Chihuahua Trough during the Aptian and Albian controlled the stratigraphic, sedimentologic and diagenetic history of the Upper Yucca Formation that outcrops in the Indio Mountains. Driven by tectonic and climatic events, and with creation of accumulation space by subsidence, a rock sequence was formed that alternated between fluvial deposits and lake sediments. In these lakes unique carbonate features (RCFs and SNCs) were formed. Field observations show that syndepositional faulting took place during the deposition of the lake sediments and fluvial deposits, and also show that the RCFs were formed in proximity to faults, while SNCs are present throughout the lake sediments (Figure 18). The lake sediments are dominated by clay, and clay bands are found within the RCFs. No coarser grained detrital material is found, which points to a setting in which detritus is not actively transported into the depocenters, (i.e. storm events are unlikely to be the cause of the banding in the RCFs). Rather, clay-rich bands represent times in which the fans grew slowly and more clay minerals could accumulate. The light oxygen isotope composition of RCFs and SNCs (average -6.55‰), and the absence of sulfate from the rocks strongly indicate that there was no contribution of marine waters to the lakes. The paleogeographic low-latitude location of deposition of the Yucca Formation to the NE of the Chihuahua Trough (Campbell, 1980), and relatively high (but fluctuating) temperatures during the Aptian (Bottini et al., 2015) indicate that the lakes of the Upper Yucca Formation were exposed to high evaporation rates, which may have led to alkaline conditions. Indeed, lake sediments from the Yucca Formation in the Southern Quitman Mountains, TX, contain Charophytes (Campbell, 1980), which are considered to be indicators of alkaline conditions (Baastrup-Spohr et al., 2013). However, the light oxygen isotope composition of the RCFs and SNCs indicate that the lakes from the Upper Yucca Formation are not typical closed lakes, because the latter display heavy oxygen

isotope signatures unless they are located in high altitude (e.g. Great Salt Lake, approximately 1280m above sea level; Figure 19), where they receive isotopically light water through precipitation. The carbon and oxygen isotope signature of the RCFs and SNCs do not show a positive correlation that is typical for closed lake systems, but at the same time a large spread in oxygen isotope compositions, which is indicative of lakes that show strong changes in their water balance. I conclude that the lakes of the Upper Yucca Formation were exposed to strong evaporation, and were supplied with water by rivers and through groundwater discharge from the fluvial sediments, as well as by fluids entering the lakes via fault systems. Recharge of the isotopically light groundwater and fault-fluids from precipitation at higher altitudes may be the reason for the light, but fluctuating oxygen isotope composition of the RCFs and SNCs. These conditions would have maintained alkaline lake conditions, which could be the explanation for the absence of tracers of animal life (i.e. skeletal grains) from the lake sediments in the study area. Microbial activity was likely not inhibited, as evidenced by the presence of stromatolites in lake bed 4. The RCFs, which were only found in lakebed 1, turned out to be an unprecedented archive of the geochemical evolution of the first lake during Upper Yucca time. Carbonate precipitation was favored by alkaline conditions caused by evaporation and the input of carbonate by the oxidation of methane at the seabed, but ultimately controlled by the input of calcium and carbonate from fluids that entered the lake along syndepositional faults, and that induced the precipitation of the fans in the vicinity of the faults.

The lakebeds from the Upper Yucca Formation are important reservoir – but not source rock – analogues for Pre-salt deposits from the South Atlantic Margin. Whereas the presence of RCFs indicates the presence of syndepositional faults that may contribute to the interconnectedness of otherwise compartmentalized reservoir blocks, the clay-rich lake sediments

(typical porosities of clay rich sediments are 0.1 to 0.4 and permeabilities are 10^{-23} to 10^{-17} m^2; Neuzil, 1994) point to the strong possibility that thin lakebeds, which may not be resolvable by seismic methods could act as impermeable seals, causing compartmentalization. Although shallow, these lakes may have been very large. Similarly, vast lakes also developed in the South Atlantic Margin where spherulites have been described in some reservoirs of Pre-Salt deposits, namely the Barra Velha Formation within the Santos Basin. The development of RCFs and spherulites, which are petrographically similar carbonate features in lake deposits: 1) reveals an analogous geologic history; 2) represents diagnostic indicators of faulting and fluid flow that enhance abiotic carbonate precipitation and; 3) provides insights into key controls on hydrocarbon reservoirs, and factors that need to be considered prior to drilling and production.

Future work in the Upper Yucca Formation should target two themes: 1) assess the size of the lakes. To date, we only know their dimensions form an essentially two-dimensional viewpoint. Identifying and correlating lakebeds to the upper panel of the stacked sheets in the research area could provide insight into this question. 2) Explore in depth the unique geochemical archive of the lakebeds, from the mineralogy of the clays, which would provide information on the paleo-climate, to the isotope geochemistry of the RCFs. With the help of such a high-resolution record, it would be possible to learn more about the dynamics of terrestrial environments during the Aptian, a time that has experienced massive, and much-debated ecological perturbations such as the Oceanic Anoxic Event 1a (Bottini et al., 2015).

9. FIGURES

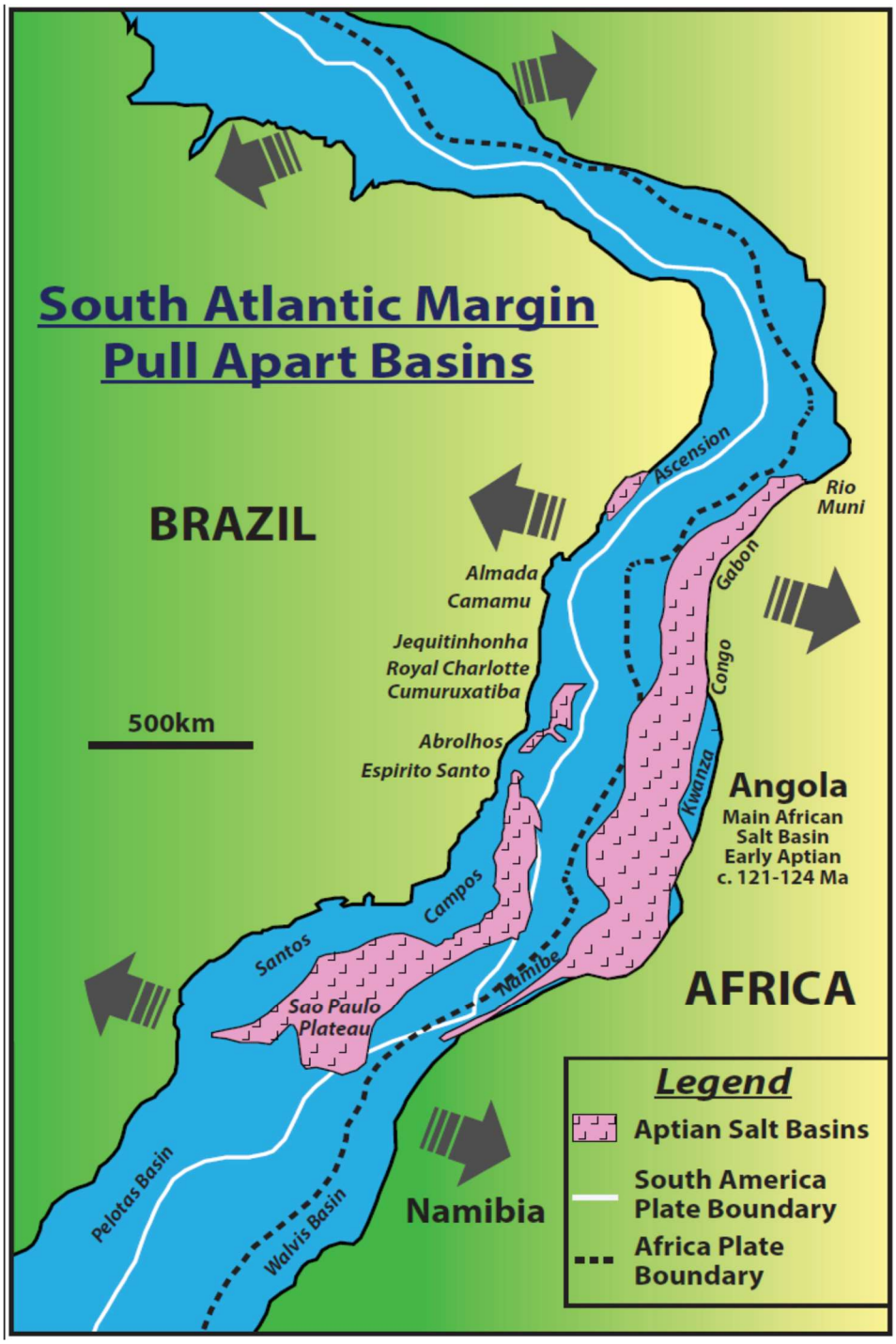

Figure 1: South Atlantic Margin pull apart basins.
Redrafted from Mohriak, 2008, modified from Davison, 2005.

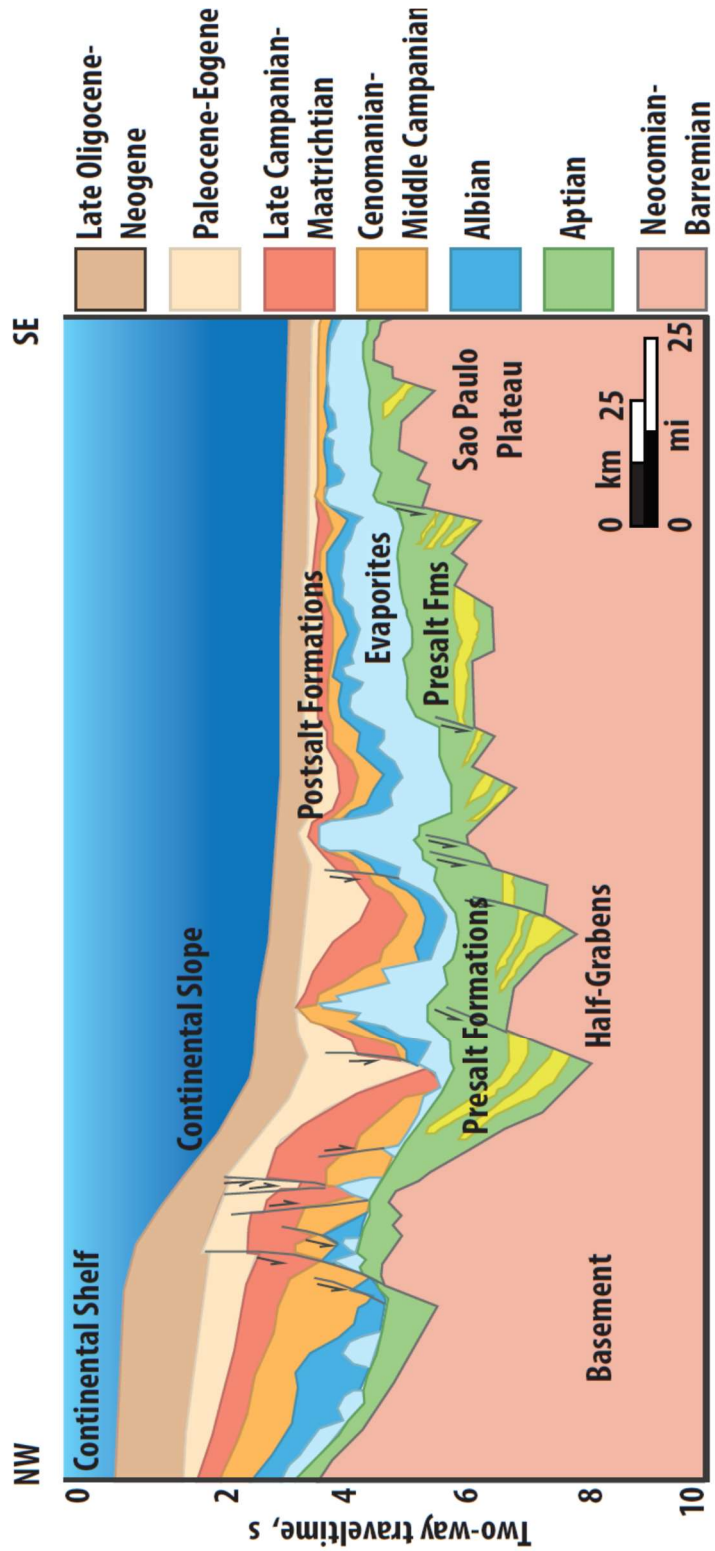

Figure 2: Cross sectional view of Santos Basin.
Presalt source rocks and carbonate reservoir formations are main targets beneath evaporites. Redrawn from Beasley et al., 2010.

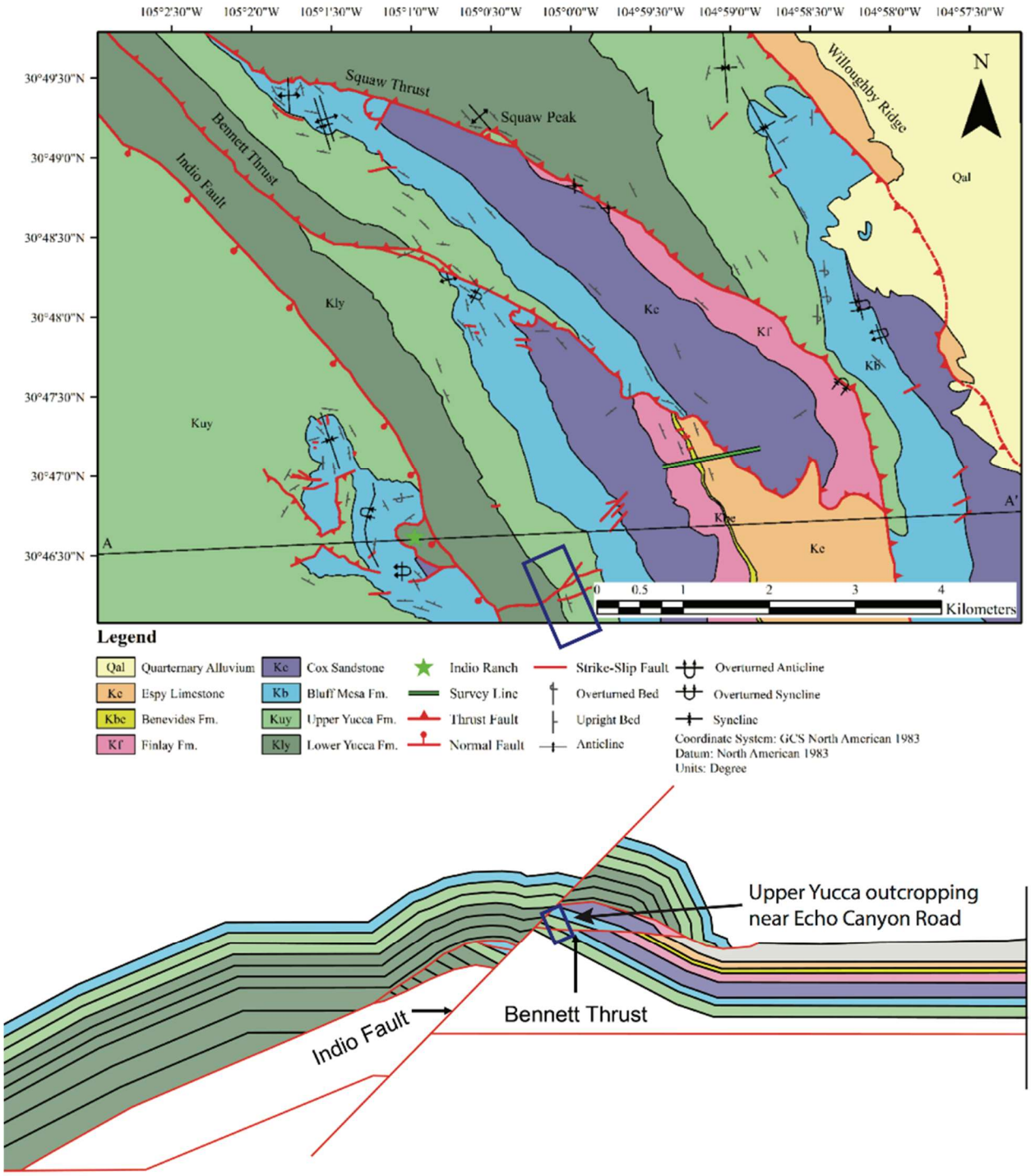

Figure 3: Geologic map of Indio Mountains.
Blue box indicates area of Upper Yucca Formation investigated in this study. (Below) Cross section interpretation of stacking panels within Indio Mountains taken from Vennemann (2017) modified after Page (2011).

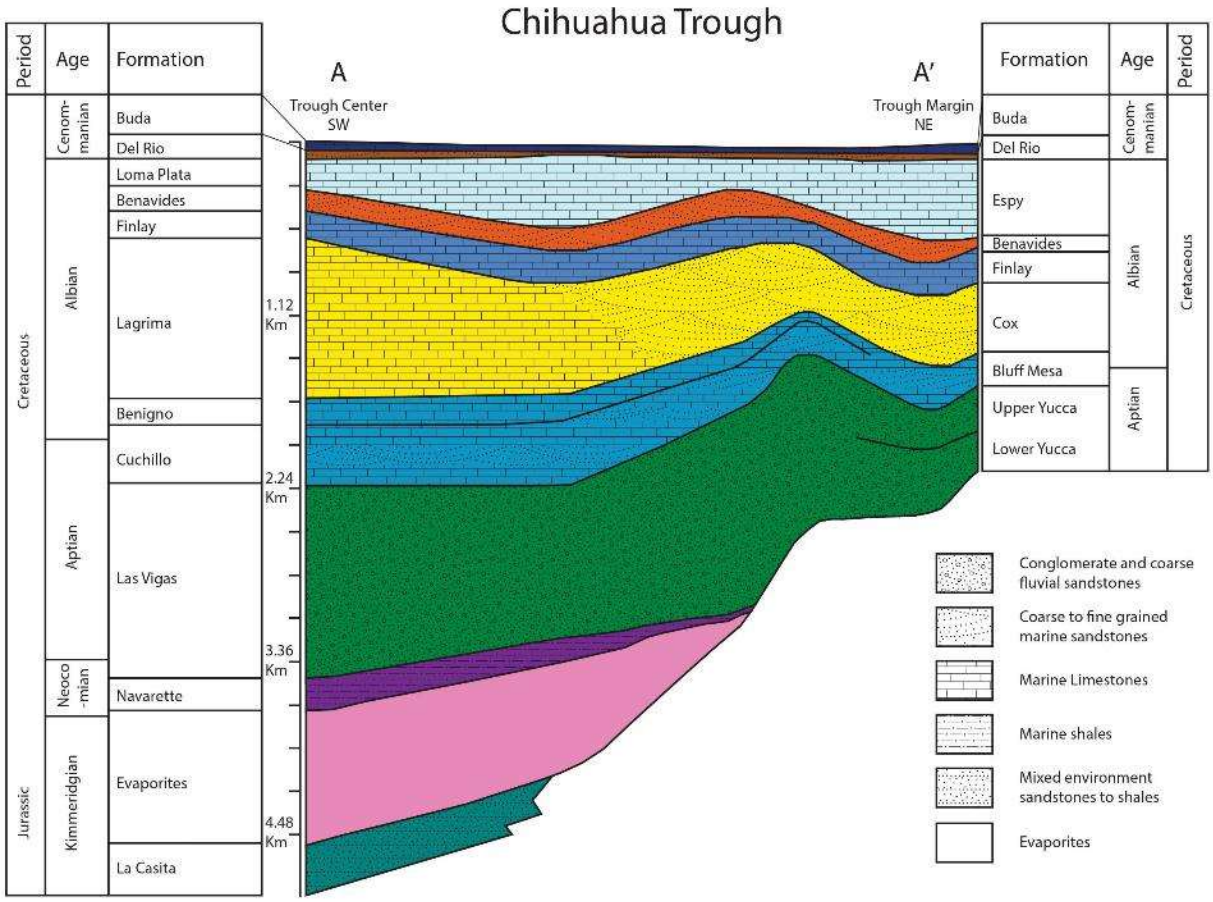

Figure 4: Cross section of Chihuahua Trough.
From Anderson (2017), Compiled from Haenggi (1970), Haenggi (2002), and Budhathoki (2013).

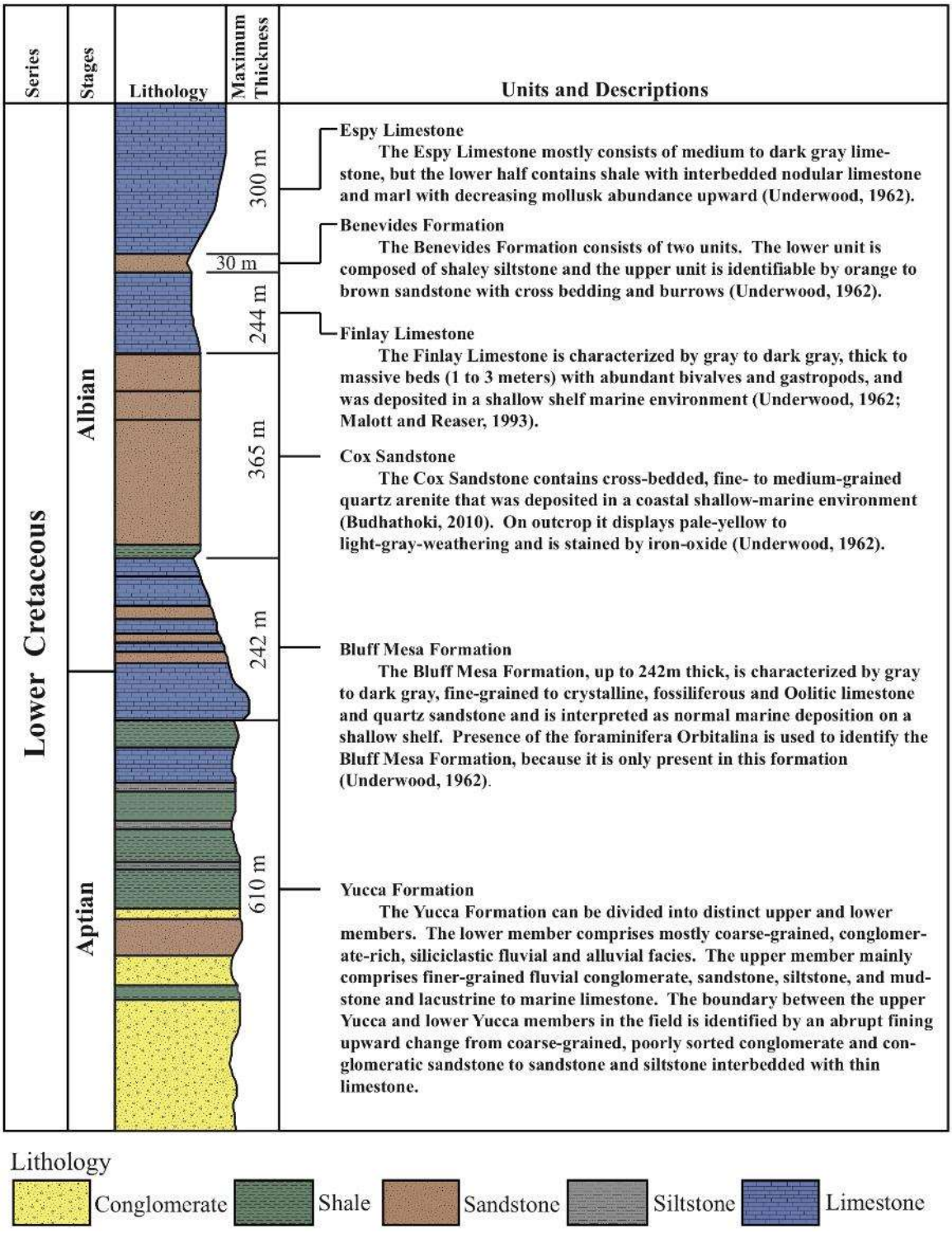

Figure 5: Simplified stratigraphic column of Indio Mountains.
Rock unit descriptions taken after Li (2014), modified from Underwood (1962).

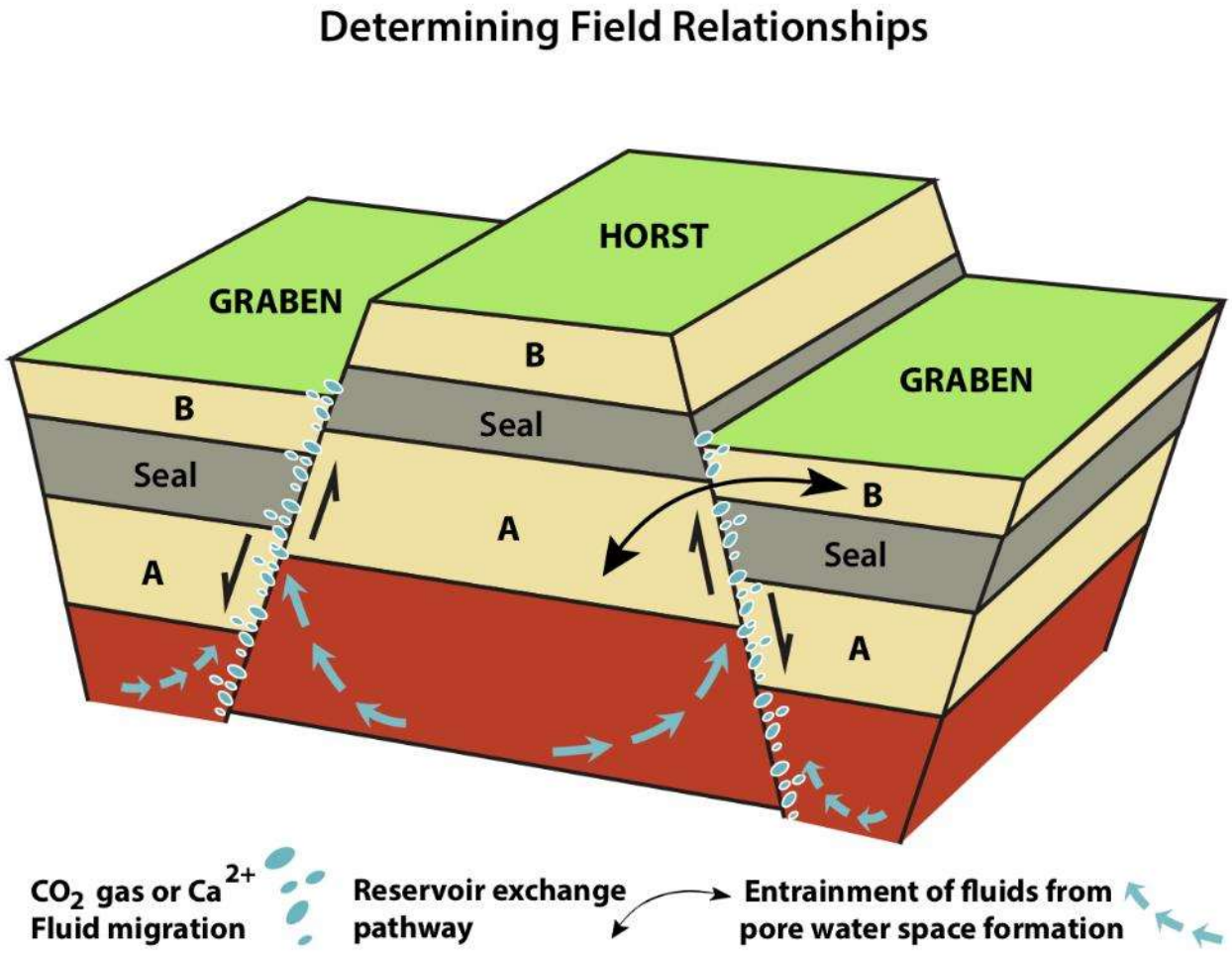

Figure 6: Simple schematic of fault and fluid migration pathways.
This sketch reflects the interconnectivity and potential reservoir seals in a faulted system.

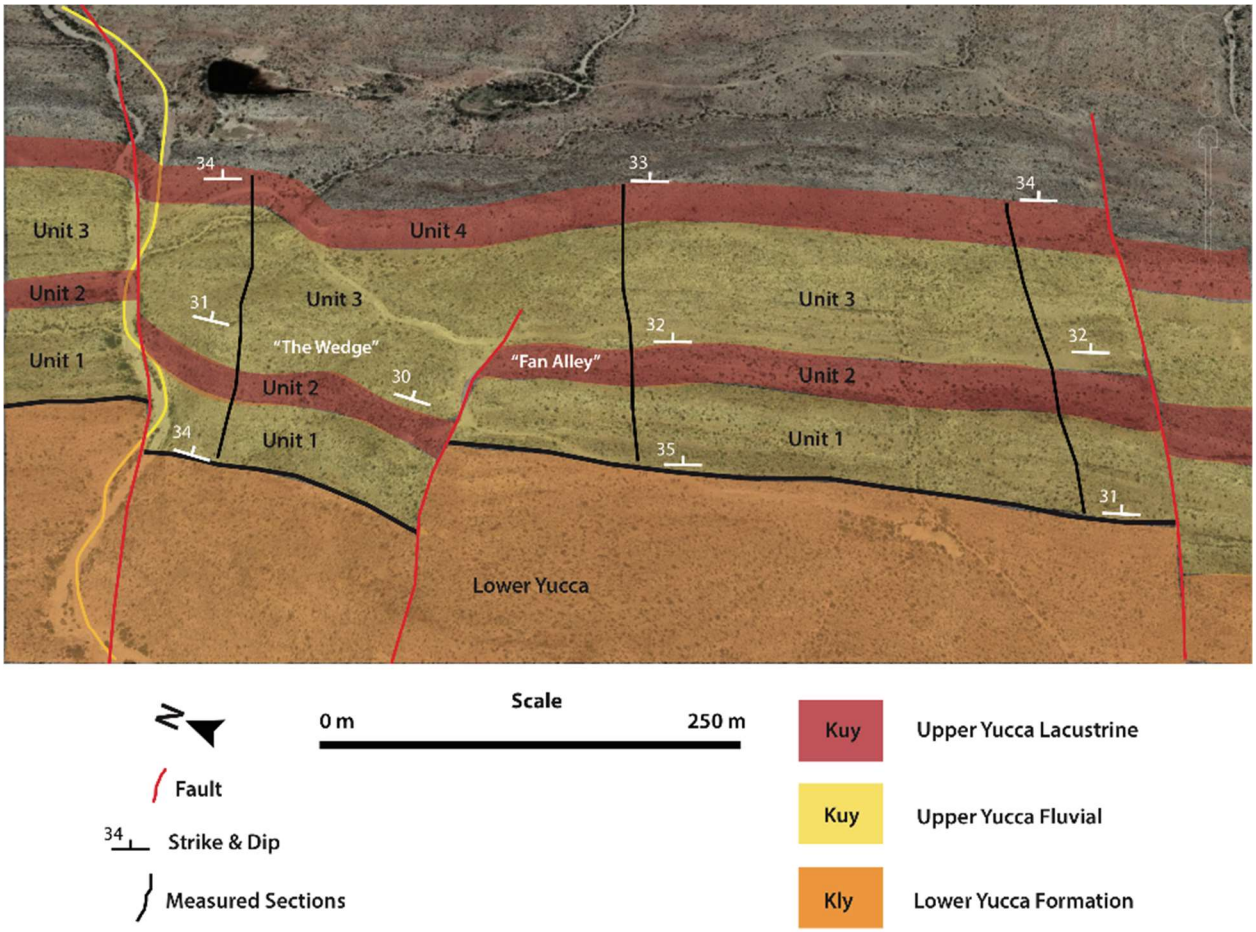

Figure 7: Detailed map of study area.
For measured sections, see Figures A1-A3.

Figure 8: 3D map of Echo Canyon study area.
With the help of 3D glasses, faults can be easily identified.

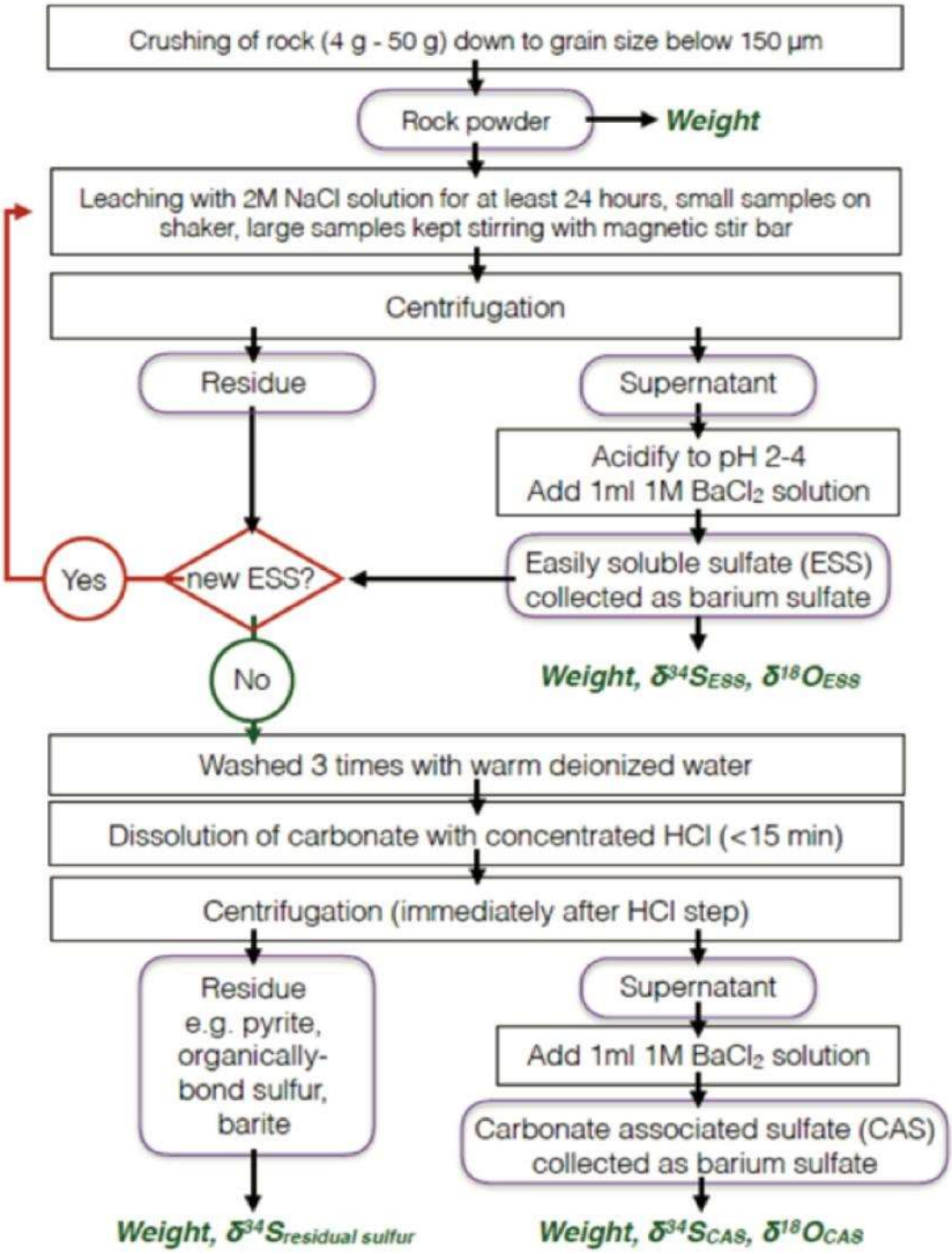

Figure 9: ESS and CAS extraction procedures.
Simplified schematic of the geochemical methodology for the extraction of sulfur phases.

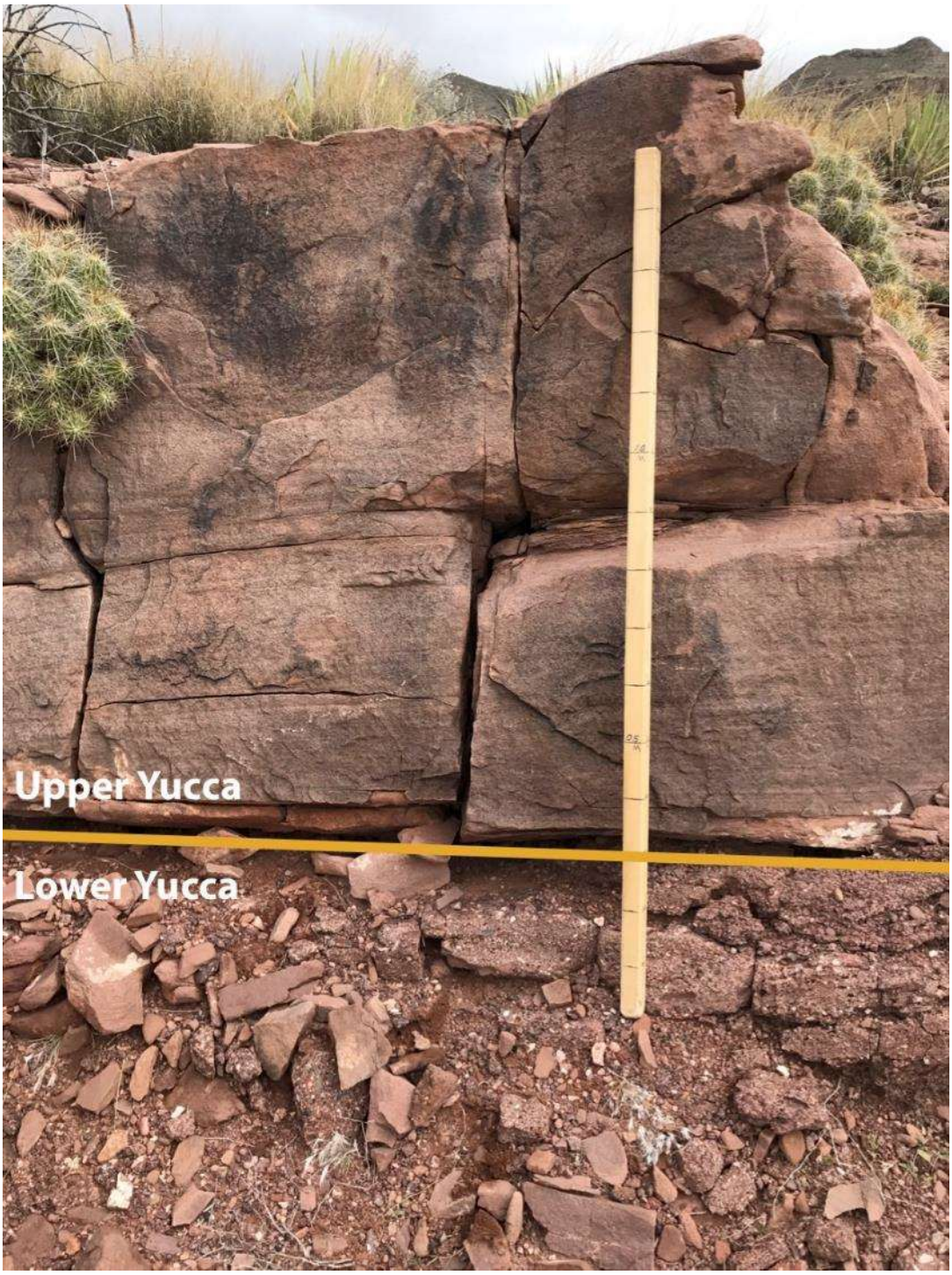

Figure 10: Unit 1 outcrop.

Figure 11: Unit 3 outcrop.

Figure 12: Unit 4 outcrop.

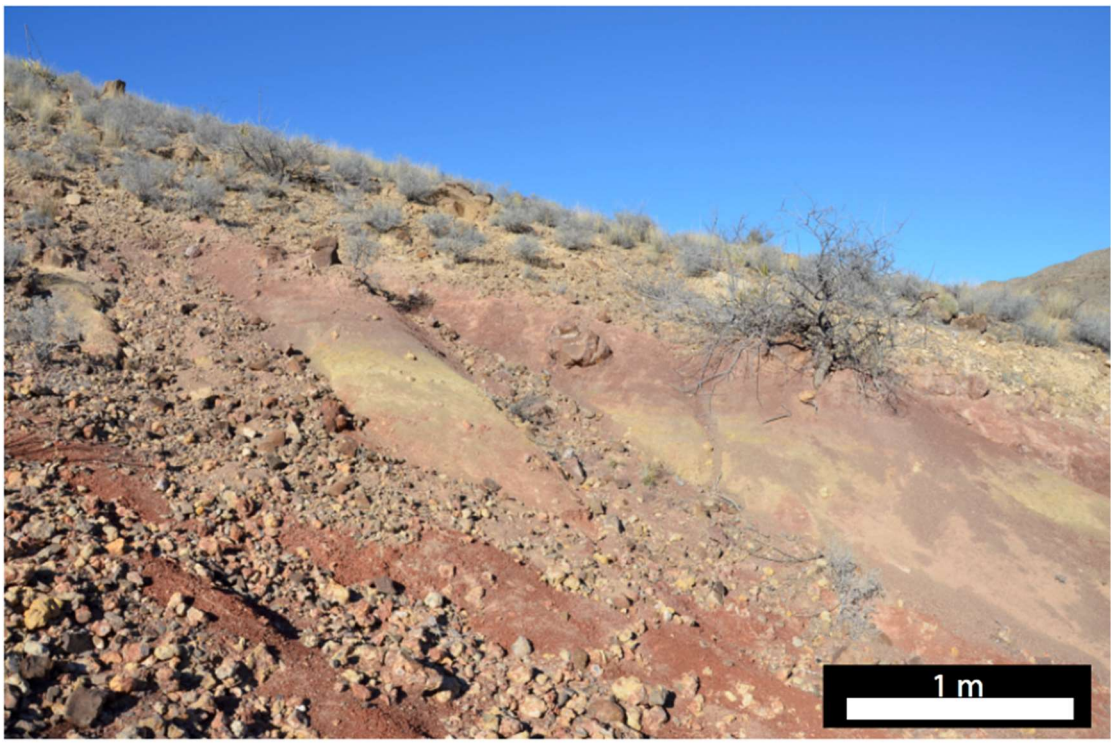

Figure 13: Photo of concretion and ‘potato beds’ outcrop.

Figure 14: Photograph of fan geochemical transects.

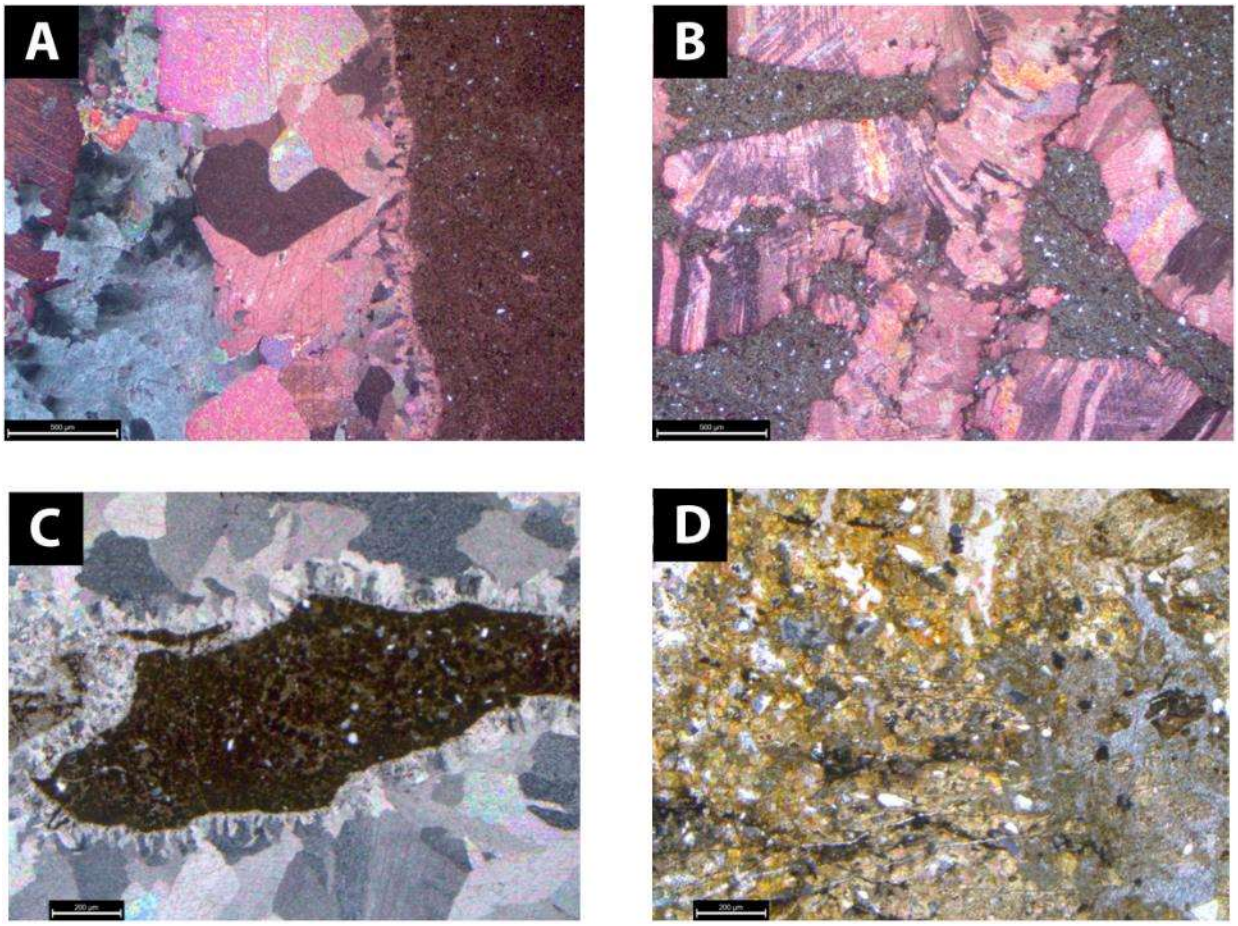

Figure 15: Thin sections of septarian nodules.
A) Septarian nodule (500 μm) that displays ferroan (iron rich) baroque dolomite (blue stain) in the cement. The cement also shows two phases of calcite; fine grained equant around the rim, and mega coarse calcite crystals towards the center. Detrital quartz grains are observed in the matrix composed of micrite. B) A septarian sample (500 μm) from the fault shows the matrix is dolomicrite cross cutting the calcite cements. C) Dead oil (left most dark stain) is trapped in this septarian matrix (200 μm). D) Sample from unit 4 (200 μm), the matrix is composed of dolomite and quartz grains. Pressure dissolution veins crosscut the matrix.

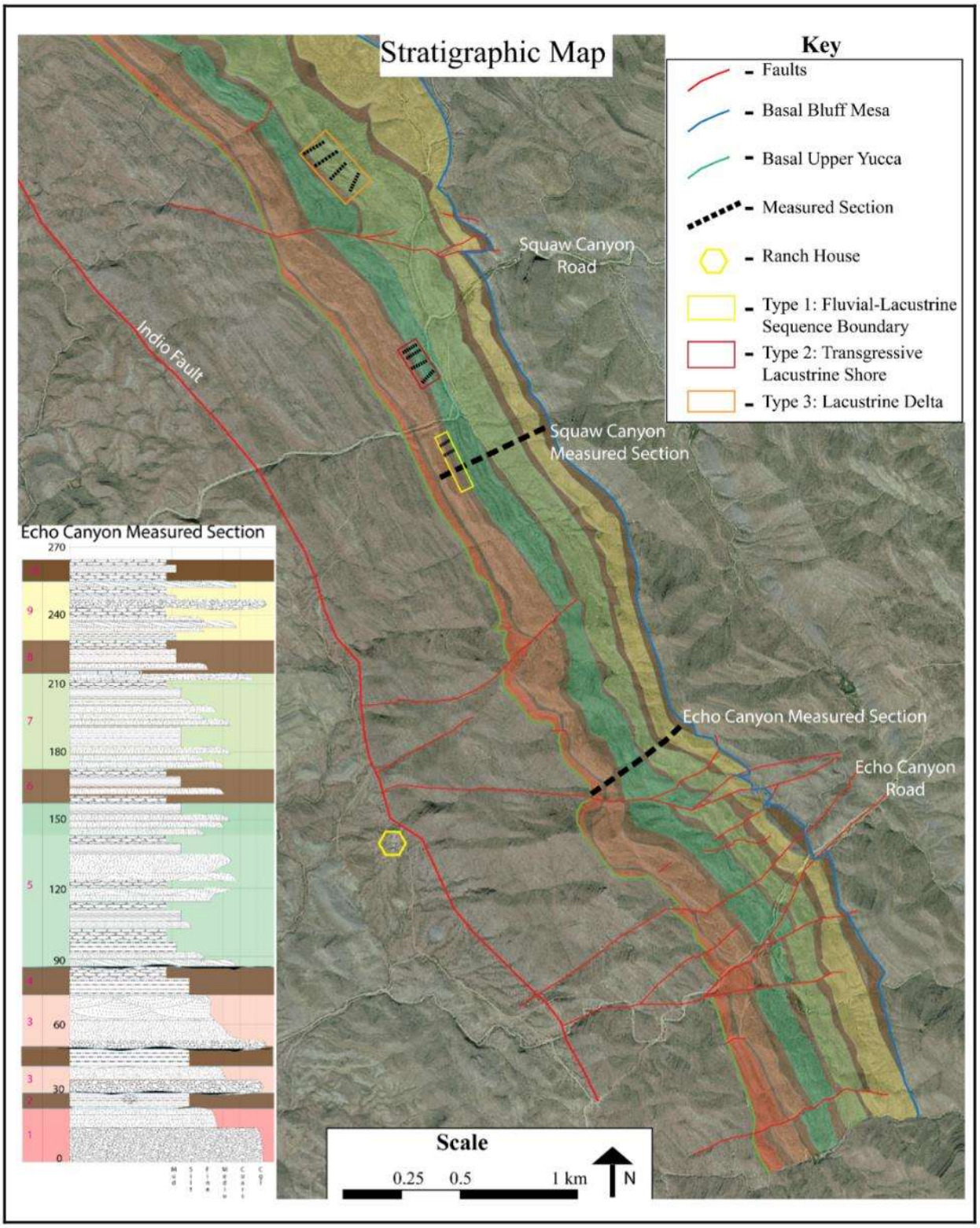

Figure 16: General stratigraphy of Upper Yucca (from Fox, 2016).
Study area is lower right portion of this figure; also indicated in Figure 18, for detailed profiles, see Figures A1-A3.

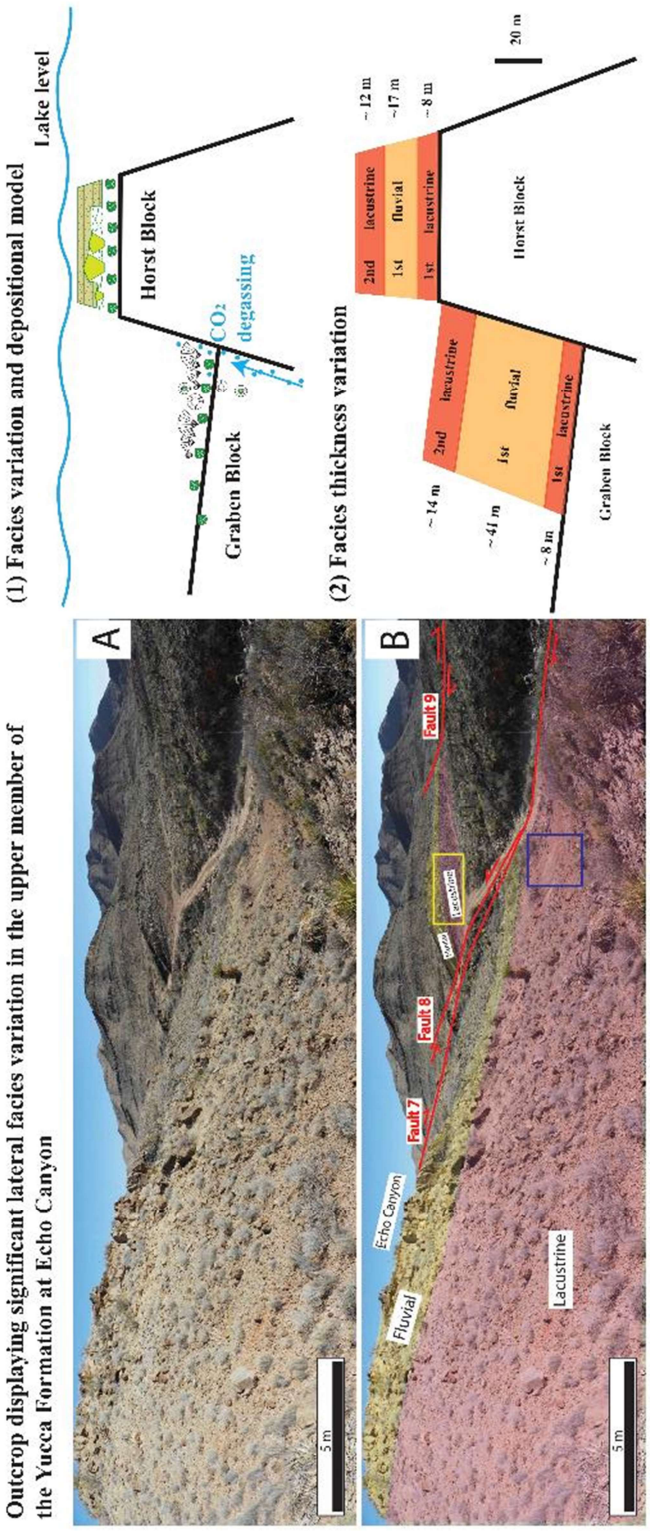

Figure 17: Previous Interpretation of Echo Canyon (Li, 2014).

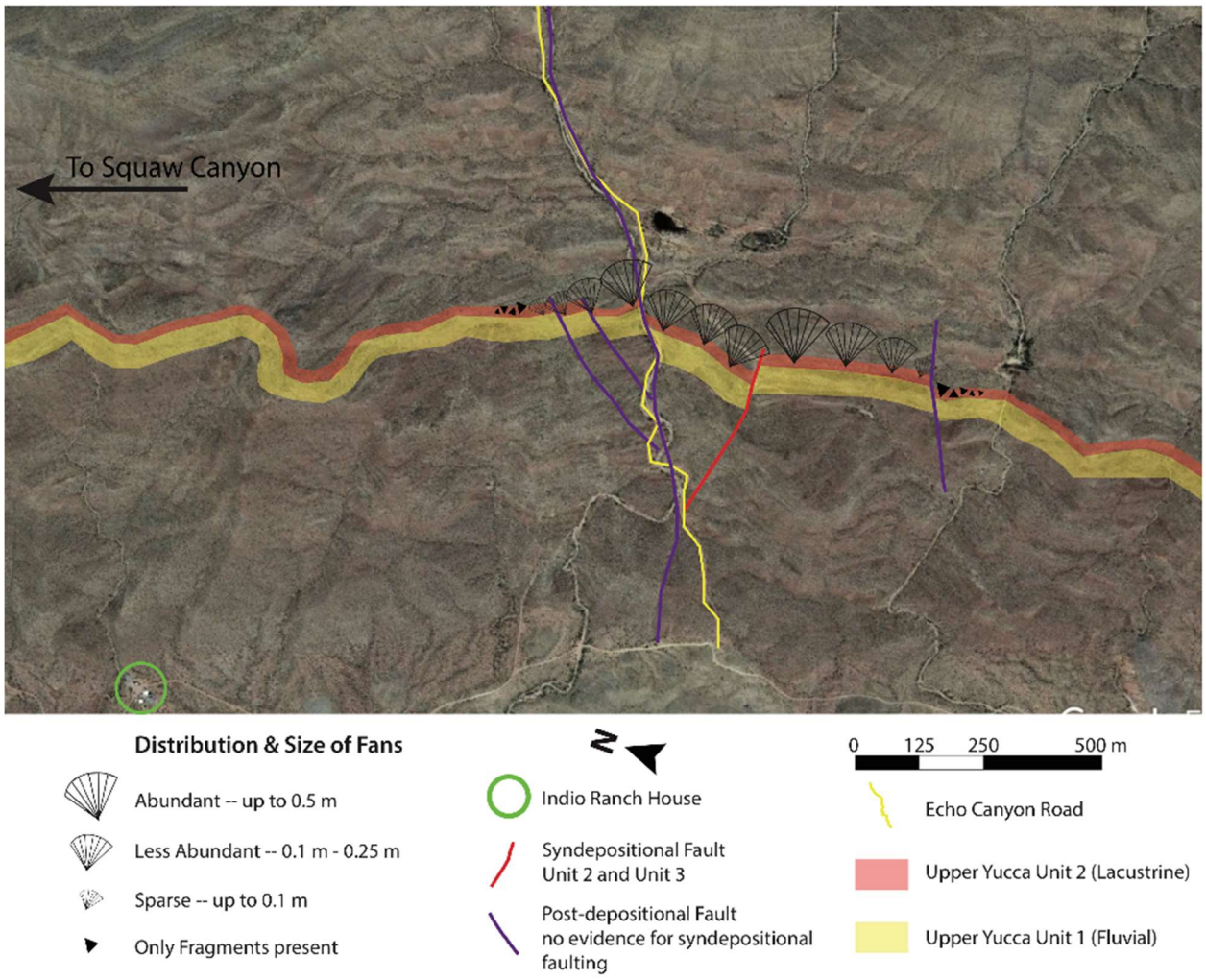

Figure 18: RCF distribution near syndepositional fault.
Abundance of RCF and size are related to proximity of syndepositional fault. Abundant represents RCFs that can be found within 2 m. Less Abundant represents RCFs every 5-10 m. Sparse represents RCFs found greater than 10 m. Extent of RCFs is approximately 500 m from fault. Unit 2 can be correlated across Squaw Canyon, roughly a distance of 5 km and nodules are present throughout.

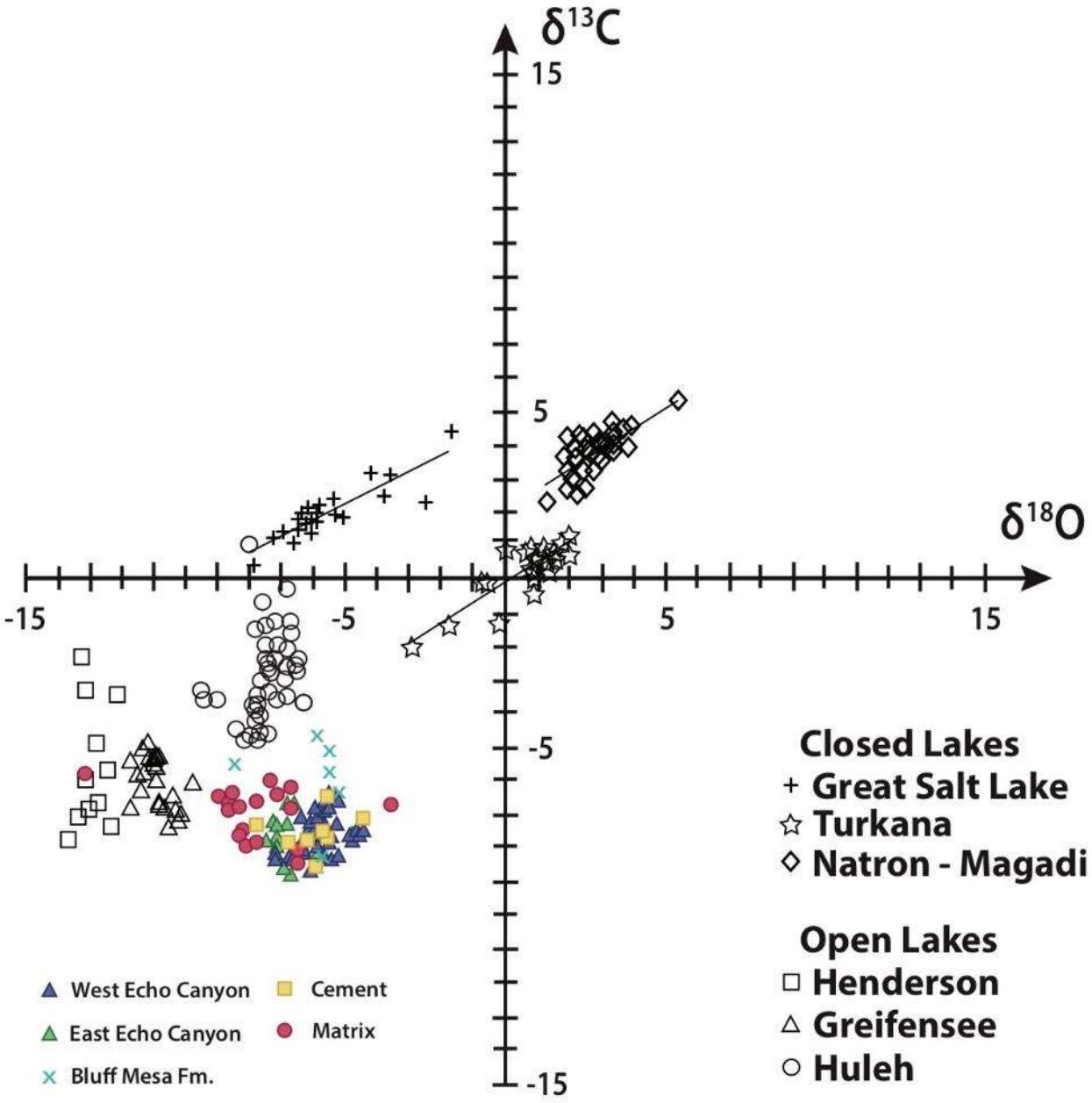

Figure 19: Typical $\delta^{13}C$ & $\delta^{18}O$ relationships for primary lacustrine carbonates.
Upper Yucca plotted with previous studies. Great salt lake data replotted from Spencer et al. (1984) and McKenzie (1985); Lake Turkana (Kenya) data from Halfman et al. (1989); Lakes Natron-Magadi (Kenya-Tanzania) data replotted from Hillaire-Marcel and Casanove (1987); Henderson Lake (US) data from Stuiver (1970); Greifensee (Switzerland) data replotted from McKenzie (1985); Lake Huleh (Israel) data replotted from Stiller and Hutchinson (1980). Carbonates from closed basins show characteristic highly correlated covariance (r normal ≥ 0.7) Modified after (Talbot and Kelts 1990)

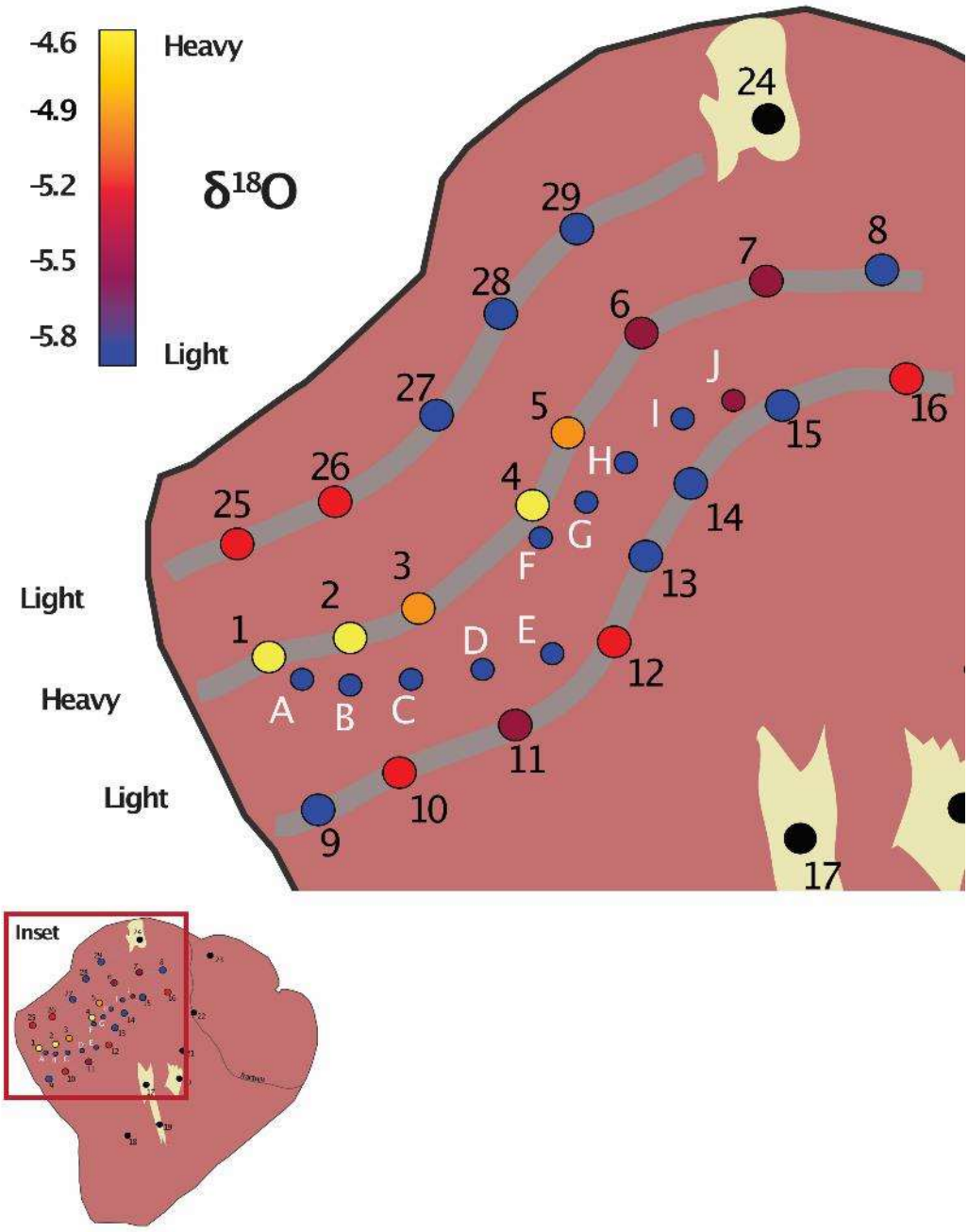

Figure 20: West Echo RCF $\delta^{18}O$ data.
Clay seams are shown in gray. Samples 1-5 have heavy $\delta^{18}O$ values. Samples 1-5 have heavy $\delta^{18}O$ values. A cyclic trend appears from inner clay seam (samples 9-16) to middle seam (samples 1-5) to outer seam (samples 25-29). Cyclicity is indicative of seasonal climate variations. Light $\delta^{18}O$ values are associated with wet seasons when lake levels were high. Heavy $\delta^{18}O$ values are associated with dry seasons when lake levels were low and evaporation of lake drove $\delta^{18}O$ values to become heavier. Size of circle indicates two different sampling campaigns, and also indicate smaller spot size sampling for higher resolution. For interpretation of trends, see text.

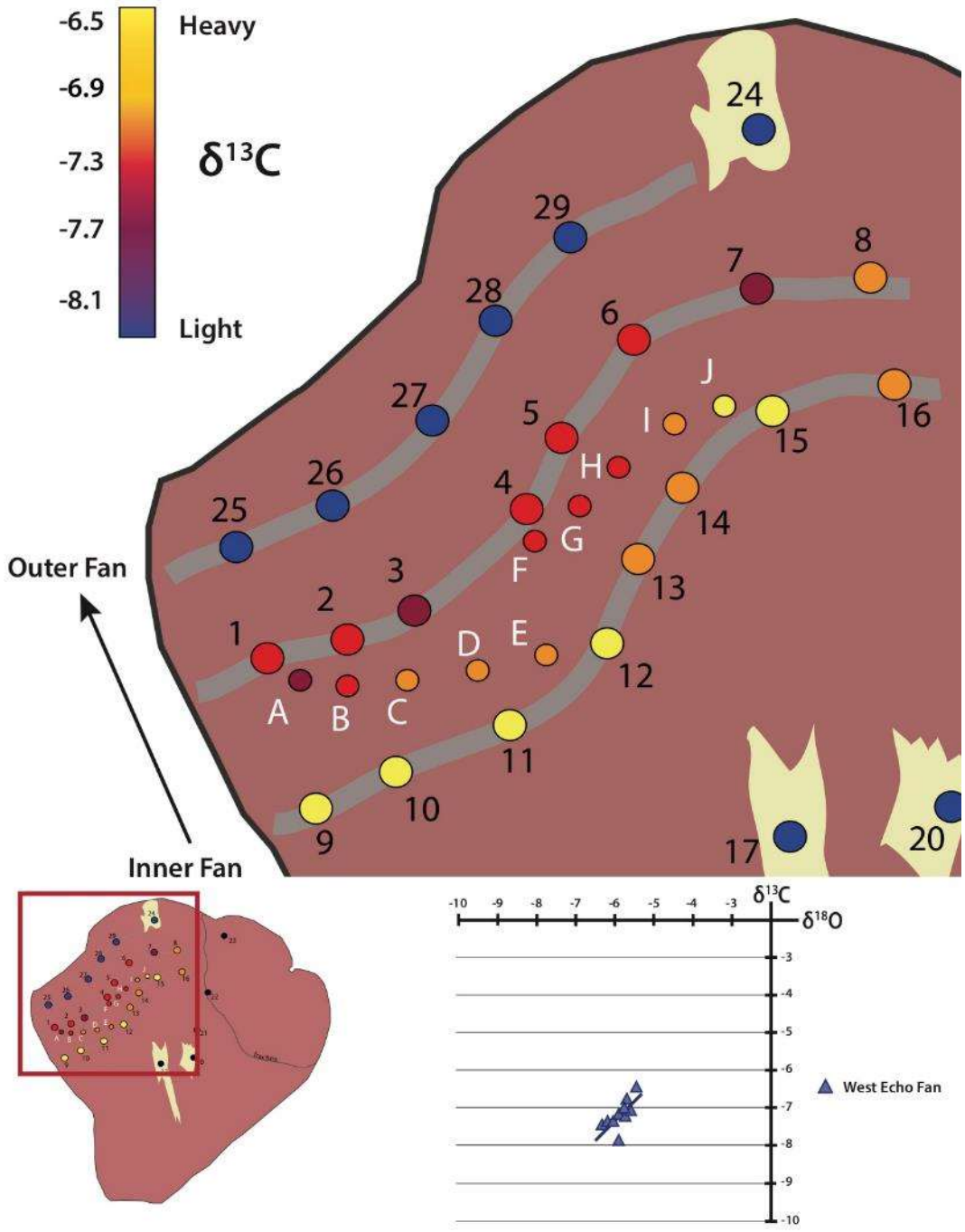

Figure 21: West Echo RCF $\delta^{13}C$ data.
Clay seams are shown in gray. A trend appears from the inner seam (samples 9-16) to the outer seam (samples 25-29). As the fan progressively formed, the lake was depleted in $\delta^{13}C$ driving values to a lighter composition. Focusing in on the graph below are samples (A-J), which is a band between the clay seams has very low clay content. I observe a positive correlation between $\delta^{13}C$ and $\delta^{18}O$, which may correspond to a time of rapid growth, also is similar to closed lake positive correlations. For interpretation of trends, see text.

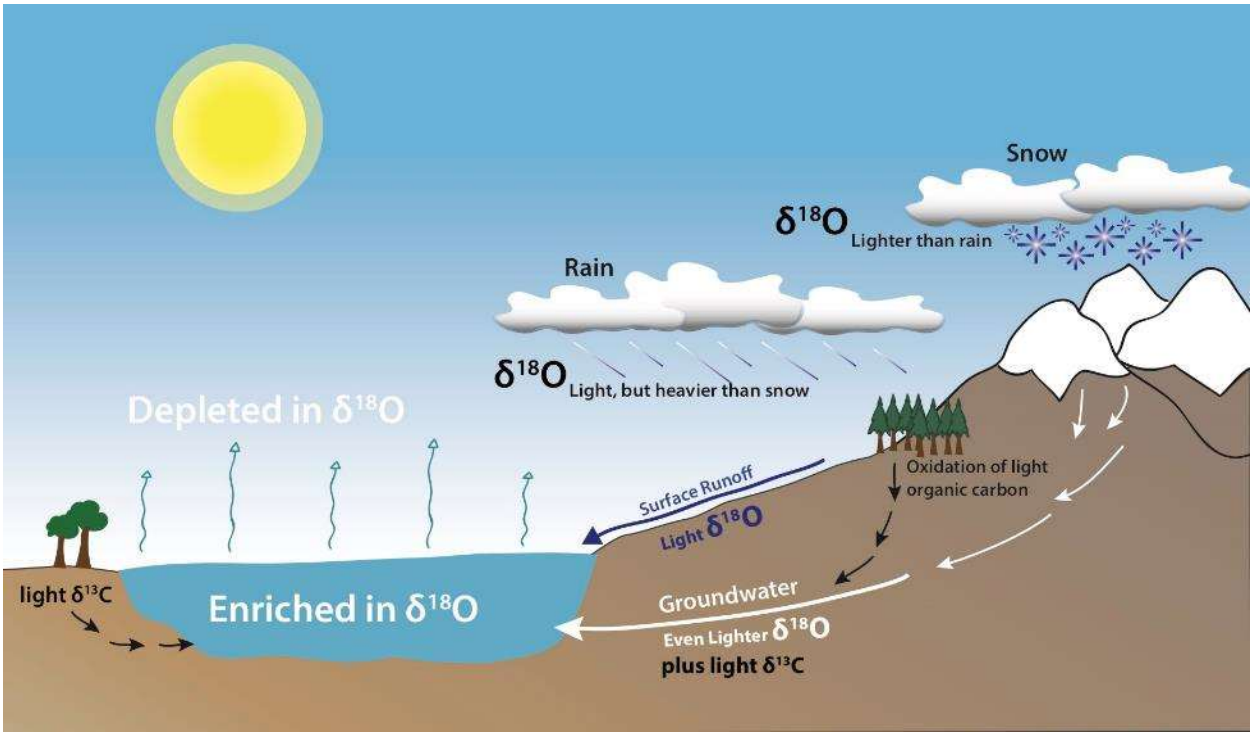

Figure 22: Model of oxygen cycle.
Simplified sketch of $\delta^{18}O$ cycle based on textbooks (e.g. Hoefs, 2008); $\delta^{18}O$ of rain is typically light but is heavier than $\delta^{18}O$ of snow. Therefore, surface runoff water has light $\delta^{18}O$, and groundwater has even lighter $\delta^{18}O$. In addition to light $\delta^{18}O$, the oxidation of organic carbon from trees and plants depletes the $\delta^{13}C$ and therefore generally lighter compositions as it travels through ground water and into the lake catchment. The lake composition is therefore enriched in $\delta^{18}O$ from surface and groundwater, but is then depleted through evaporation.

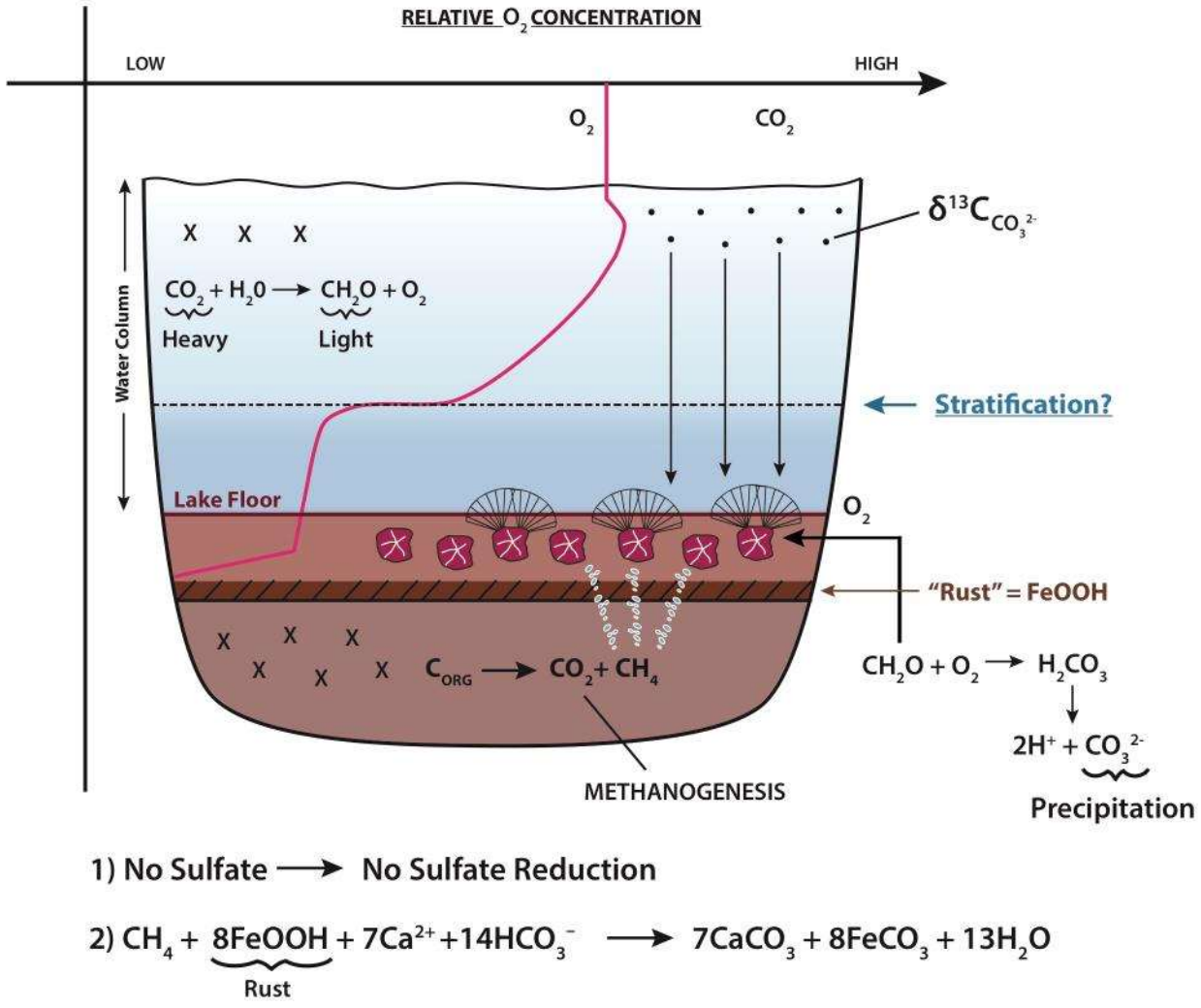

Figure 23: Illustration of Upper Yucca lake geochemical drivers.
Drivers lead to $\delta^{13}C$ and $\delta^{18}O$ values found in Radial Carbonate Fans (RCFs) and Septarian Nodule Concretions (SNCs).

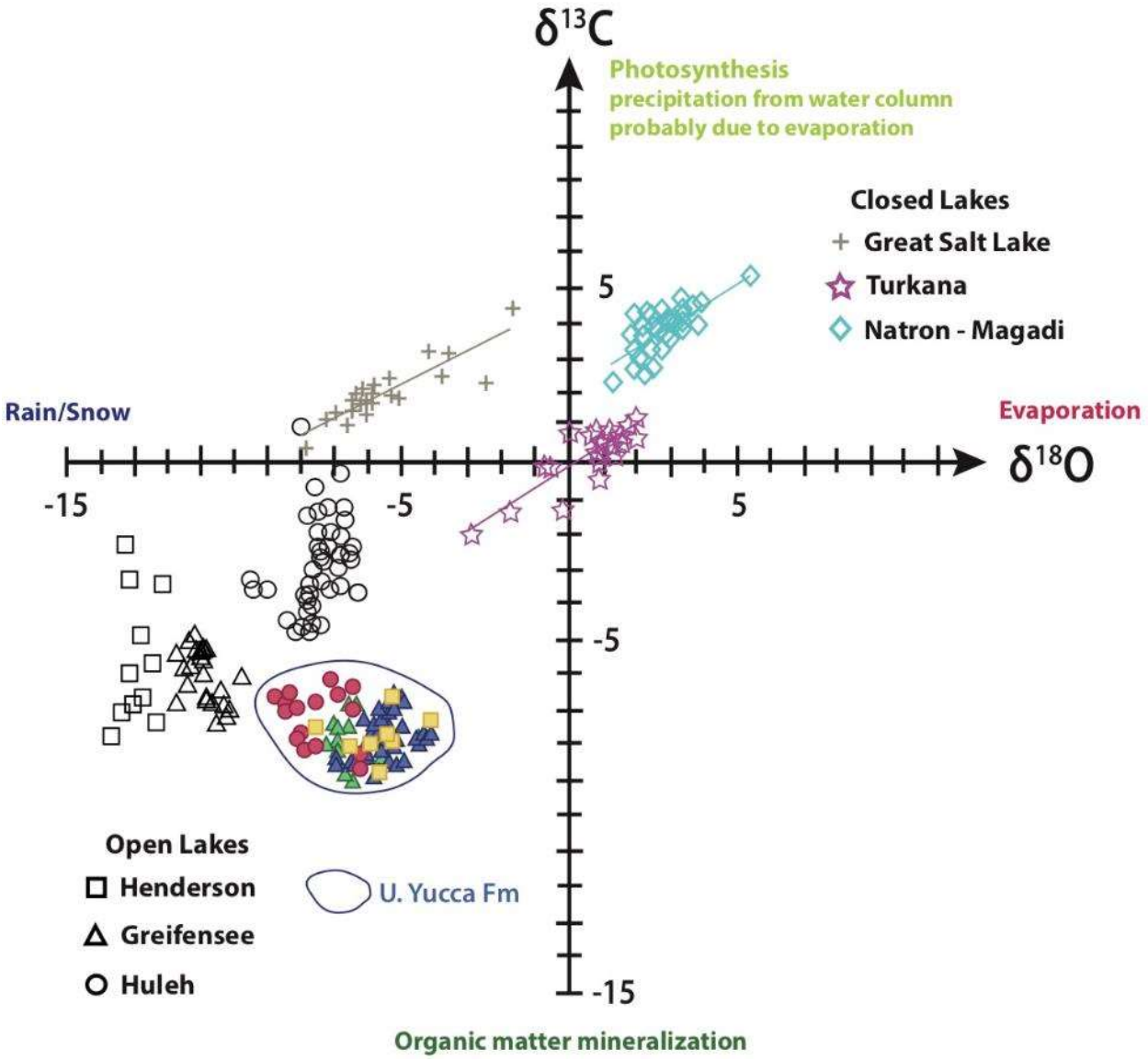

Figure 24: Possible mechanisms for closed lakes and open lakes.
$\delta^{13}C$ and $\delta^{18}O$ values are compared between closed lakes and open lakes along with Upper Yucca values obtained from this study. Possible mechanisms that drive $\delta^{13}C$ and $\delta^{18}O$ values to a heavy or light state include: photosynthesis (top), evaporation (right), organic matter mineralization (bottom), and rain/snow input (left.) Closed lakes have positive $\delta^{13}C$ and $\delta^{18}O$ correlation trends that can be linked through evaporation (Talbot and Kelts, 1990). Open lakes are independent where different mechanisms influence both $\delta^{13}C$ and $\delta^{18}O$ values therefore do not have a correlation. $\delta^{13}C$ values are dynamic and show wide ranges indicating that several different environments impact lake carbonates.

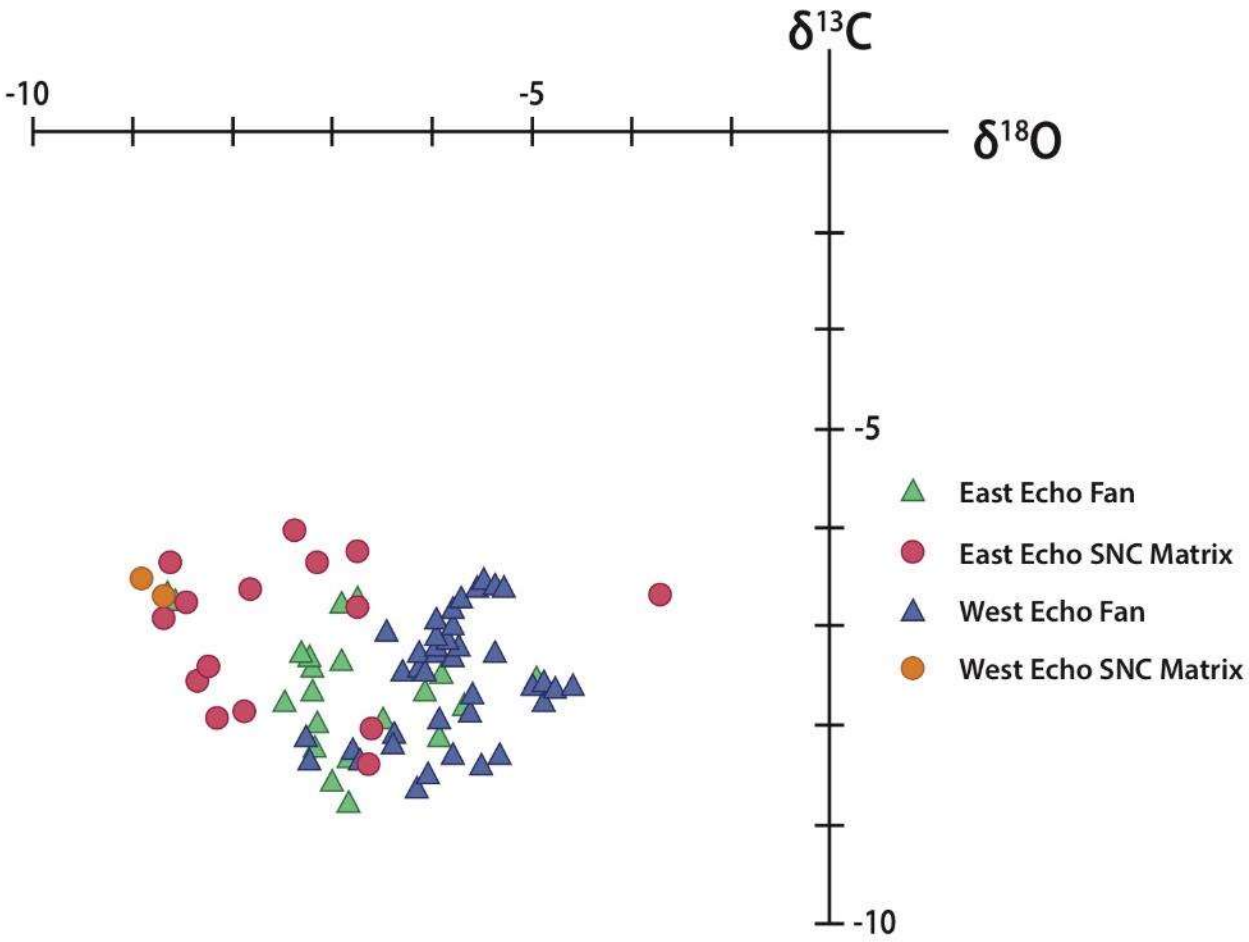

Figure 25: Upper Yucca RCF and SNC $\delta^{13}C$ and $\delta^{18}O$ comparison.

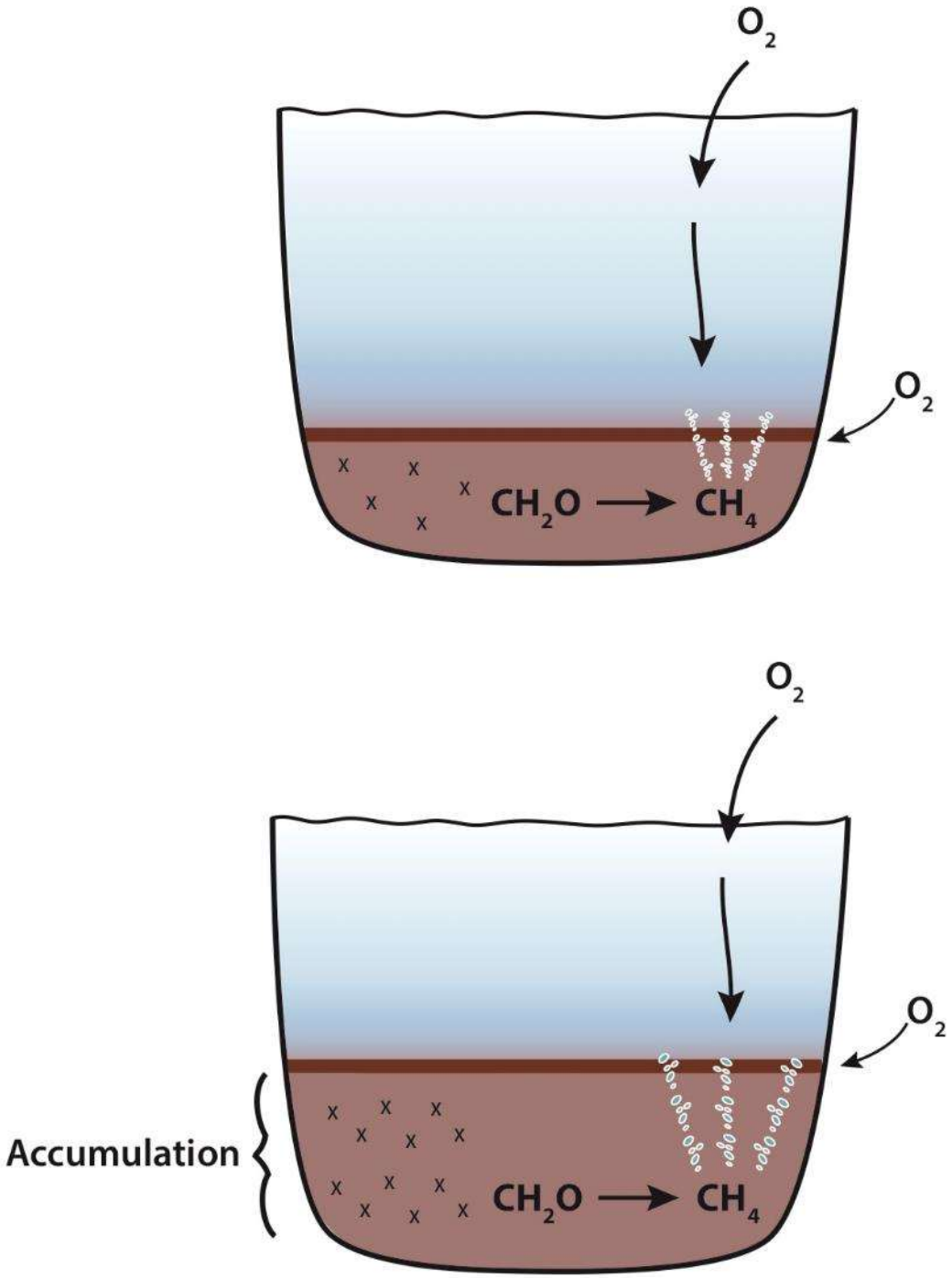

Figure 26: Profile of lake accumulation sediments result in more methane degassing.

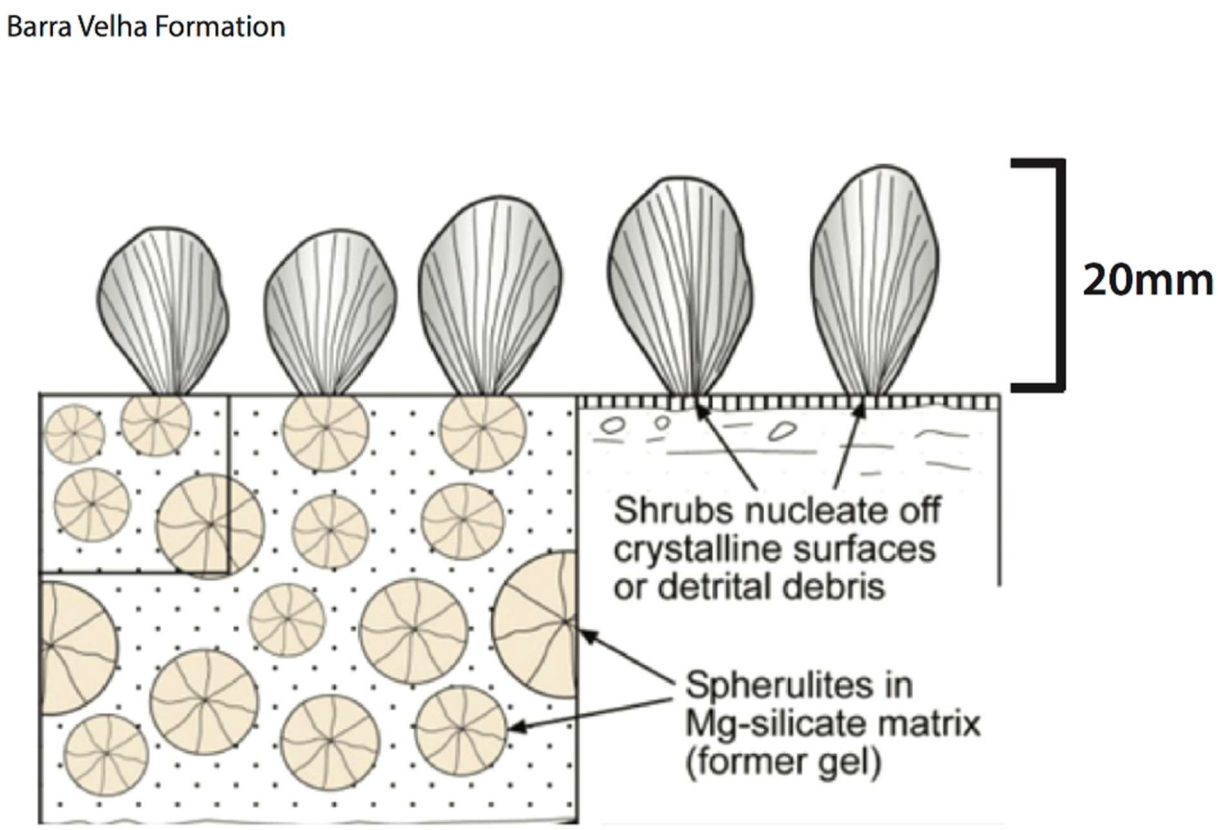

Figure 27: Comparison of Upper Yucca features with Barra Velha Formation, Santos Basin.
If scale of shrubs and spherulites from the Barra Velha Formation would be increased by a factor of 10, the features would look similar to the RCFs and SNCs.

REFERENCES

Al-Droubi, A., Fritz, B., Gac, J.Y., and Tardy, Y., 1980, Generalized residual alkalinity concept; application to prediction of the chemical evolution of natural waters by evaporation: American Journal of Science, v. 280, p. 560–572, doi: 10.2475/ajs.280.6.560.

Alessandretti, L., Warren, L.V., Machado, R., Novello, V.F., and Sayeg, I.J., 2015, Septarian carbonate concretions in the Permian Rio do Rasto Formation: Birth, growth and implications for the early diagenetic history of southwestern Gondwana succession: Sedimentary Geology, v. 326, p. 1–15, doi: 10.1016/j.sedgeo.2015.06.007.

Anderson, A., 2017, Depositional Controls and Sequence Stratigraphy of Lacustrine to Marine-Transgressive Deposits in a Rift Basin, Lower Cretaceous Bluff Mesa, Indio Mountains, West Texas. [M.S.]: The University of Texas at El Paso, 180 p.

Astin, T.R. Septarian Crack Formation in Carbonate Concretions from Shales and Mudstones:, http://www.minersoc.org/pages/Archive-CM/Volume_21/21-4-617.pdf (accessed April 2016).

Awramik, S.M., and Buchheim, H.P., 2012, The Quest for Microbialite Analogs to the South Atlantic Pre-Salt Carbonate Hydrocarbon Reservoirs of Africa and South America: v. 55, p. 21–27.

Baastrup-Spohr, L., Iversen, L.L., Dahl-Nielsen, J., and Sand-Jensen, K., 2013, Seventy years of changes in the abundance of Danish charophytes: Freshwater Biology, v. 58, p. 1682–1693, doi: 10.1111/fwb.12159.

Beasley, C.J., Fiduk, J.C., Bize, E., Boyd, A., Frydman, M., Zerilli, A., Dribus, J.R., Moreira, J.L.P., and Pinto, A.C.C., 2010, Brazil's Presalt Play: Oilfield Review, v. 22, p. 28–37.

Beltrao, R.L.C., Sombra, C.L., Lage, A.C.V.M., Netto, J.R.F., and Henriques, C.C.D., 2009, SS: Pre-salt Santos basin - Challenges and New Technologies for the Development of the Pre-salt Cluster, Santos Basin, Brazil, *in* Offshore Technology Conference, doi: 10.4043/19880-MS.

Bemis, S.P., Micklethwaite, S., Turner, D., James, M.R., Akciz, S., Thiele, S.T., and Bangash, H.A., 2014, Ground-based and UAV-Based photogrammetry: A multi-scale, high-resolution mapping tool for structural geology and paleoseismology: Journal of Structural Geology, v. 69, Part A, p. 163–178, doi: 10.1016/j.jsg.2014.10.007.

Bergersen, E., 2016, Geochemical signatures as a chemostratigraphic tool to correlate stacked carbonates of the Glorieta, Victorio Peak, Cutoff, and Upper San Andres Formations West Dog Canyon, Guadalupe Mountains, New Mexico [M.S.]: The University of Texas at El Paso, 112 p.

Bird, P., 1998, Kinematic history of the Laramide orogeny in latitudes 35°–49°N, western United States: Tectonics, v. 17, p. 780–801, doi: 10.1029/98TC02698.

Blaich, O.A., Faleide, J.I., and Tsikalas, F., 2011, Crustal breakup and continent-ocean transition at South Atlantic conjugate margins: Journal of Geophysical Research: Solid Earth, v. 116, p. B01402, doi: 10.1029/2010JB007686.

Bosence, D., Gibbons, K., Heron, D.P.L., Morgan, W.A., Pritchard, T., and Vining, B.A., 2015, Microbial carbonates in space and time: introduction: Geological Society, London, Special Publications, v. 418, p. SP418.14, doi: 10.1144/SP418.14.

Bottini, C., Erba, E., Tiraboschi, D., Jenkyns, H.C., Schouten, S., and Sinninghe Damsté, J.S., 2015, Climate variability and ocean fertility during the Aptian Stage: Climate of the Past, v. 11, p. 383–402, doi: 10.5194/cp-11-383-2015.

Bruhn, C.H.L., Gomes, J.A.T., Lucchese, D., Jr, C., and Johann, P.R.S., 2003, Campos Basin: Reservoir Characterization and Management - Historical Overview and Future Challenges, *in* Offshore Technology Conference, doi: 10.4043/15220-MS.

Burne, R.V., and Moore, L.S., 1987, Microbialites; organosedimentary deposits of benthic microbial communities: PALAIOS, v. 2, p. 241–254, doi: 10.2307/3514674.

Campbell, D.H., 1980, The Yucca Formation-Early Cretaceous continental and transitional environments, southern Quitman Mountains, Hudspeth County, Texas, *in* Trans-Pecos region: New Mexico Geol. Soc. Guidebook, 31st Field Conf, p. 159–168.

Chopra, S., Castagna, J., and Portniaguine, O., 2006, Seismic resolution and thin-bed reflectivity inversion: CSEG recorder, v. 31, p. 19–25.

Clayton, R.N., and Degens, E.T., 1959, Use of Carbon Isotope Analyses of Carbonates for Differentiating Fresh-Water and Marine Sediments: GEOLOGICAL NOTES: AAPG Bulletin, v. 43, p. 890–897.

DeFord, R.K., 1964, *in* History of geologic exploration in Chihuahua, in Geology of Mine Plomosas-Placer de Guadalupe area, Chihuahua, Mexico, West Texas Geological Society, West Texas Geological Society, Field Trip Guidebook.

Dias, J.L., 2005, Tectônica, estratigrafia e sedimentação no Andar Aptiano da margem leste brasileira: Boletim de Geociências da PETROBRAS, v. 13, p. 7–25.

Dickson, W., Schiefelbein, C.F., Odegard, M.E., and Zumberge, J.E., 2016, Petroleum systems asymmetry across the South Atlantic Equatorial Margins: Geological Society, London, Special Publications, v. 431, p. SP431.13, doi: 10.1144/SP431.13.

Dorobek, S., Piccoli, L., Coffey, B., and Adams, A., 2012, Carbonate Rock-Forming Processes in the Pre-salt “Sag” Successions of Campos Basin, Offshore Brazil: Evidence for Seasonal, Dominantly Abiotic Carbonate Precipitation, Substrate Controls, and Broader Geologic Implications: AAPG Search and Discovery Article, v. 90153, p. 1–2.

Droxler, A.W., Khana, P., and Lehrman, D.J., 2014, Growth Phases in the Upper Cambrian Wilberns Microbial Reef Evolution (Mason County, Texas): 2014 AAPG Annual Convention and Exhibition, v. AAPG Search and Discovery article 90189.

Flügel, E., 2010, New Perspectives in Microfacies, *in* Microfacies of Carbonate Rocks, Springer, Berlin, Heidelberg, p. 1–6, doi: 10.1007/978-3-642-03796-2_1.

Fox, M.R., 2016, Sedimentologic and stratigraphic analysis of synrift siliciclastic fluvial and lacustrine strata in the Lower Cretaceous upper Yucca Formation, Indio Mountains, West Ttexas [M.S.]: The University of Texas at El Paso, 149 p., https://0-search-proquest-com.lib.utep.edu/pqdtglobal/docview/1834819739/abstract/7742B372913147C4PQ/1.

Gischler, E., Heindel, K., Birgel, D., Brunner, B., Reitner, J., and Peckmann, J., 2017, Cryptic biostalactites in a submerged karst cave of the Belize Barrier Reef revisited: Pendant bioconstructions cemented by microbial micrite: Palaeogeography, Palaeoclimatology, Palaeoecology, v. 468, p. 34–51, doi: 10.1016/j.palaeo.2016.11.042.

Haenggi, W.T., 2002, Tectonic history of the Chihuahua trough, Mexico and adjacient USA, Part II: Mesozoic and Cenozoic: Boletin de la Sociedad Geologica Mexicana, v. Tomo LV, p. 38–94.

Hamon, Y., Rohais, S., Deschamps, R., and Gasparrini, M., 2012, Outcrop analogue of Pre-salt microbial series from South Atlantic: the Yacoraite Fm, Salta rift system (NW Argentina): AAPG Search and Discovery Article, v. 90153, p. 1–2.

Hoefs, J., 2008, Stable isotope geochemistry: Springer Science & Business Media.

Jahnert, R.J., and Collins, L.B., 2012, Characteristics, distribution and morphogenesis of subtidal microbial systems in Shark Bay, Australia: Marine Geology, v. 303–306, p. 115–136, doi: 10.1016/j.margeo.2012.02.009.

Jahnert, R.J., and Collins, L.B., 2011, Significance of subtidal microbial deposits in Shark Bay, Australia: Marine Geology, v. 286, p. 106–111, doi: 10.1016/j.margeo.2011.05.006.

Leng, M.J., and Marshall, J.D., 2004, Palaeoclimate interpretation of stable isotope data from lake sediment archives: Quaternary Science Reviews, v. 23, p. 811–831, doi: 10.1016/j.quascirev.2003.06.012.

Li, X., 2014, Sedimentologic, stratigraphic, and diagenetic analysis of microbialite-bearing lacustrine rift sequence within the Lower Cretaceous Yucca Formation, Indio Mountains, West Texas [M.S.]: The University of Texas at El Paso, 153 p., http://search.proquest.com/docview/1615419559/abstract?accountid=7121 (accessed February 2015).

Marcano, G., Anka, Z., and di Primio, R., 2013, Major controlling factors on hydrocarbon generation and leakage in South Atlantic conjugate margins: A comparative study of Colorado, Orange, Campos and Lower Congo basins: Tectonophysics, v. 604, p. 172–190, doi: 10.1016/j.tecto.2013.02.004.

McCaffrey, K.J.W., Jones, R.R., Holdsworth, R.E., Wilson, R.W., Clegg, P., Imber, J., Holliman, N., and Trinks, I., 2005, Unlocking the spatial dimension: digital technologies and the future of geoscience fieldwork: Journal of the Geological Society, v. 162, p. 927–938, doi: 10.1144/0016-764905-017.

Montelongo, M., 2017, A New Method for Ultra-Low Sulfate Extraction and a Pilot Study in Arid Soils [M.S.]: The University of Texas at El Paso, 89 p.

Monty, C., and Hardie, L., 1976, .6 The Geological Significance of the Freshwater Blue-Green Algal Calcareous Marsh: Developments in sedimentology, v. 20, p. 447–477.

Neuzil, C.E., 1994, How permeable are clays and shales? Water Resources Research, v. 30, p. 145–150, doi: 10.1029/93WR02930.

Page, S.J., 2011, Fold-thrust system overprinting syn-rift structures on the margin of an inverted rift basin: Indio mountains, west Texas [Master Thesis]: The University of Texas at El Paso, 60 p.

Pavlis, T.L., and Mason, K.A., 2017, The New World of 3D Geologic Mapping: GSA Today, p. 4–10, doi: 10.1130/GSATG313A.1.

Petersohn, E., Abelha, M., and Pedrosa, L., 2013, Brasil Pre-Salt.

Platt, and Wright, 1991, Lacustrine carbonate: facies models, facies distributions and hydrocarbon aspects, *in* P. Anado, L. Cabrera, and K. Kelts eds., Lacustrine Facies Analysis, IAS Special Publication, v. 13, p. 57–74.

Riding, R., 2008, Abiogenic, microbial and hybrid authigenic carbonate crusts: components of Precambrian stromatolites: Geologia Croatica, v. 61, p. 73–103.

Riding, R., 2000, Microbial carbonates: the geological record of calcified bacterial–algal mats and biofilms: Sedimentology, v. 47, p. 179–214, doi: 10.1046/j.1365-3091.2000.00003.x.

Seard, C., Camoin, G., Rouchy, J.-M., and Virgone, A., 2013, Composition, structure and evolution of a lacustrine carbonate margin dominated by microbialites: Case study from the Green River formation (Eocene; Wyoming, USA): Palaeogeography, Palaeoclimatology, Palaeoecology, v. 381–382, p. 128–144, doi: 10.1016/j.palaeo.2013.04.023.

Talbot, M.R., and Kelts, K., 1990, Paleolimnological Signatures from Carbon and Oxygen Isotopic Ratios in Carbonates, from Organic Carbon-Rich Lacustrine Sediments: Chapter 6: v. 133, p. 99–112.

Terra, G., Spadini, A., Franca, A., and Sombra, C., 2010, Carbonate rock classification applied to Brazilian sedimentary basins: Boletin Geociencias Petrobras, v. 18, p. 9–29.

Tosca, N.J., and Wright, V.P., 2015, Diagenetic pathways linked to labile Mg-clays in lacustrine carbonate reservoirs: a model for the origin of secondary porosity in the Cretaceous pre-salt Barra Velha Formation, offshore Brazil: Geological Society, London, Special Publications, doi: 10.1144/SP435.1.

Underwood, J.R., 1962, Geology of the Eagle Mountains and Vicinity, Hudspeth County, Texas: Dissertation: The University of Texas at Austin, 560 p.

Wotte, T., Shields-Zhou, G.A., and Strauss, H., 2012, Carbonate-associated sulfate: Experimental comparisons of common extraction methods and recommendations toward a standard analytical protocol: Chemical Geology, v. 326–327, p. 132–144, doi: 10.1016/j.chemgeo.2012.07.020.

Wright, V.P., and Barnett, A.J., 2015, An abiotic model for the development of textures in some South Atlantic early Cretaceous lacustrine carbonates: Geological Society, London, Special Publications, v. 418, p. SP418.3, doi: 10.1144/SP418.3.

Ziegenbalg, S.B., Brunner, B., Rouchy, J.M., Birgel, D., Pierre, C., Böttcher, M.E., Caruso, A., Immenhauser, A., and Peckmann, J., 2010, Formation of secondary carbonates and native sulphur in sulphate-rich Messinian strata, Sicily: Sedimentary Geology, v. 227, p. 37–50, doi: 10.1016/j.sedgeo.2010.03.007.

APPENDIX – MEASURED SECTION DETAILS

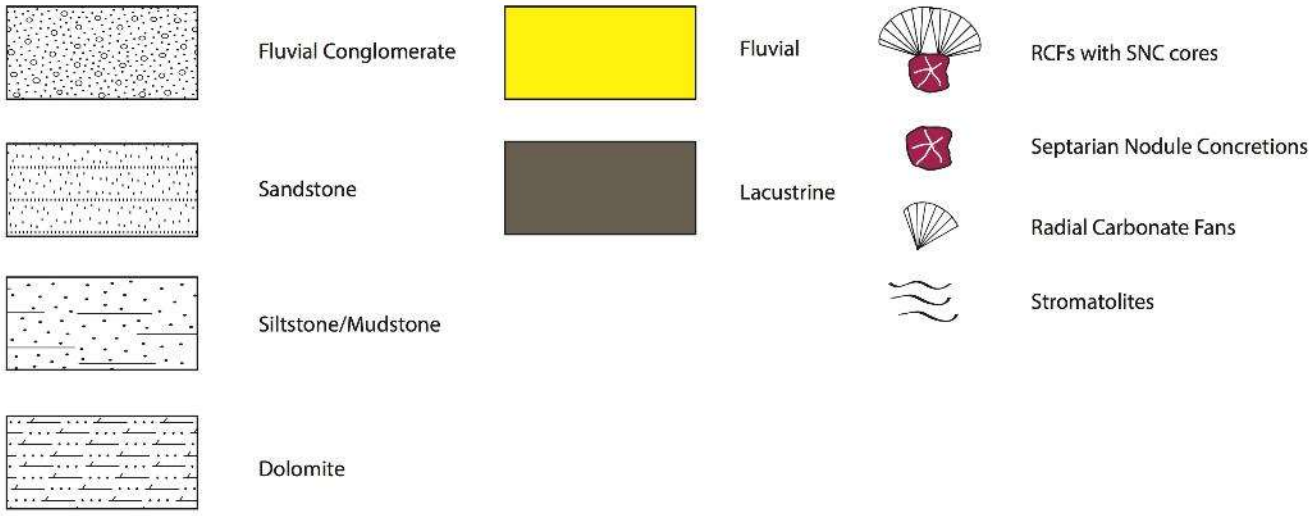

Legend for Appendix Figures A1 – A3.

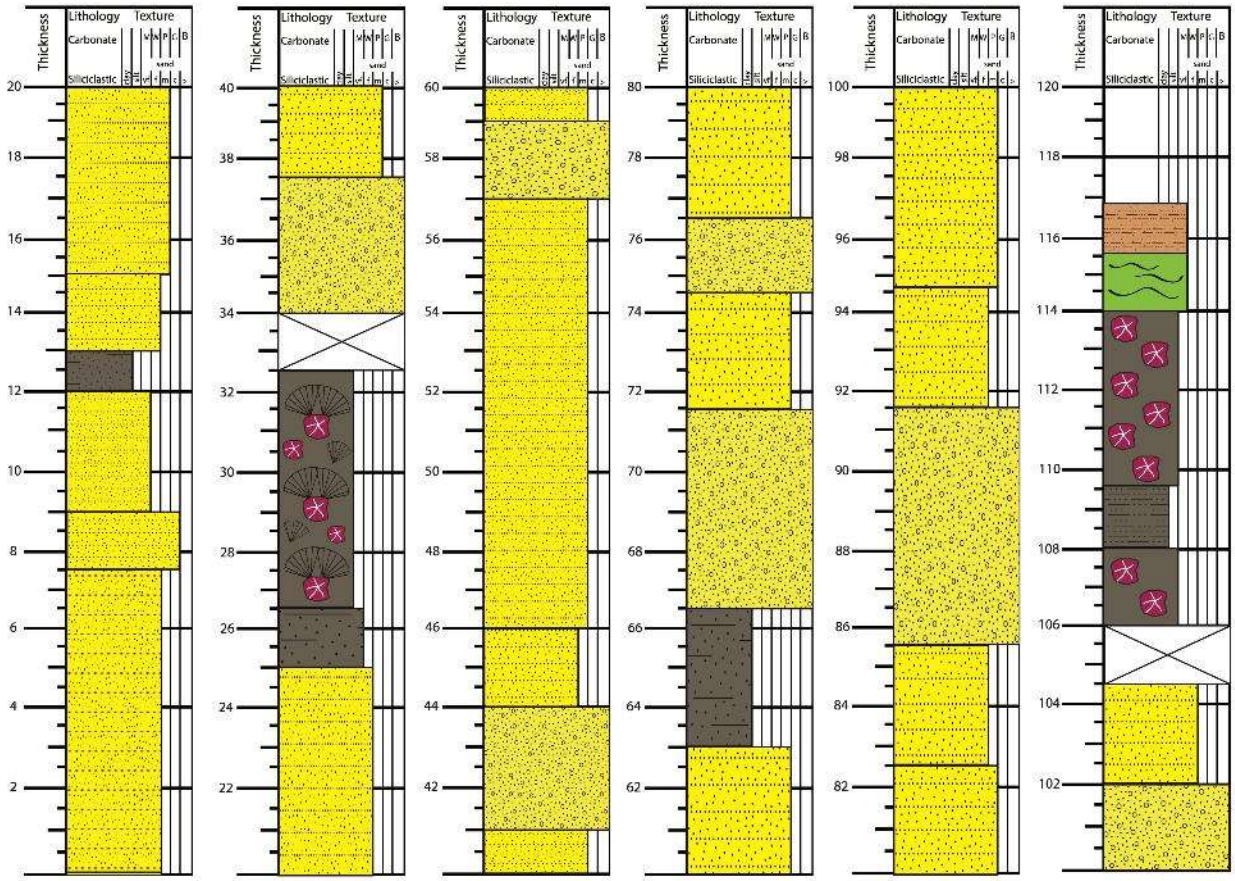

Figure A1. Detailed measured section for section directly adjacent to Echo Canyon Rd.

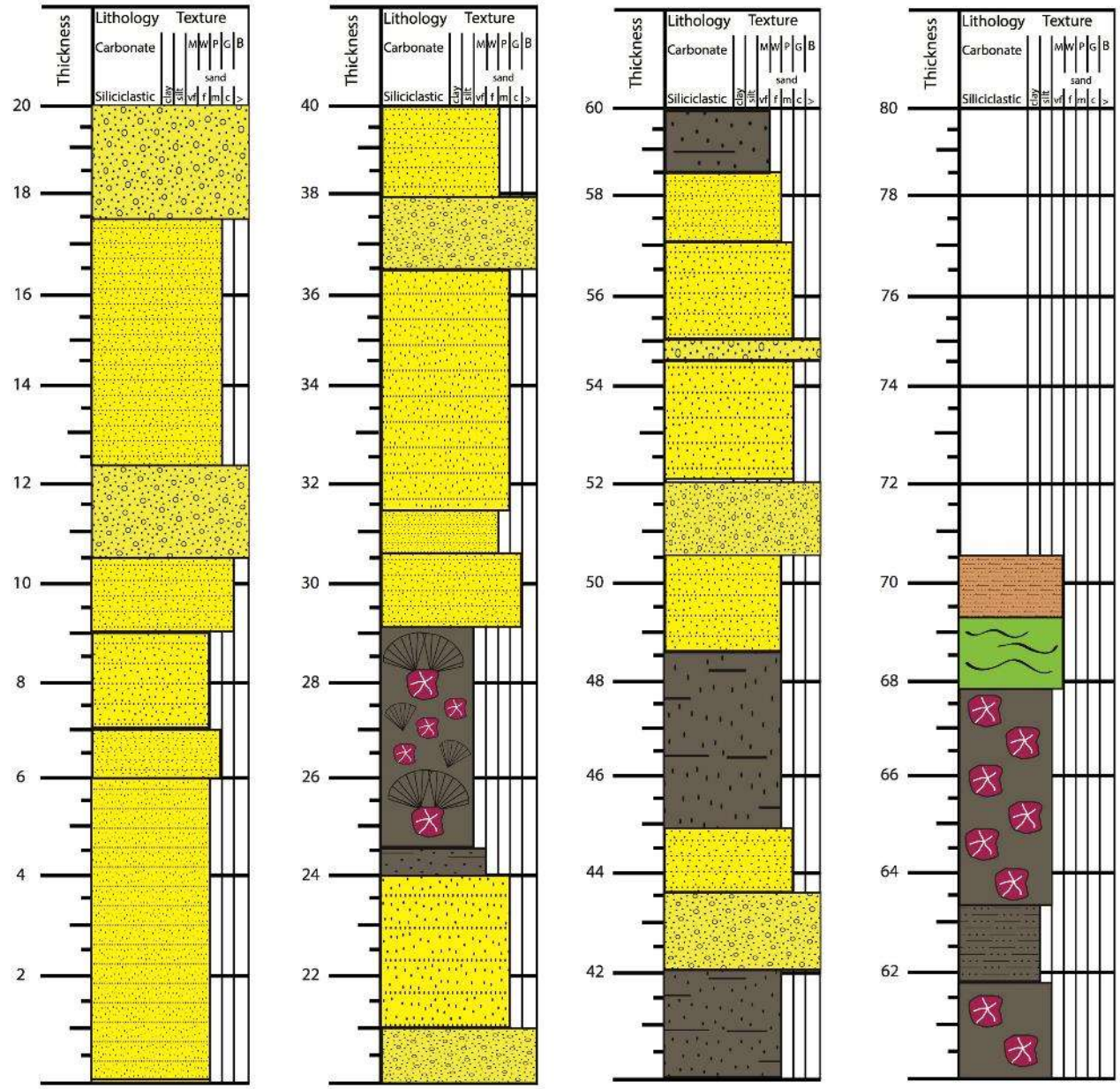

Figure A2. Detailed measured section for center section of study.

Figure A3. Detailed measured section for furthest southeast section of study area.

VITA

Andre Armando Llanos was born and raised in Northeast El Paso, and always loved looking up at the Franklin Mountains from his home. Upon graduating 4th in his class from Andress High School he attended UT Austin to study Aerospace Engineering. His ambitions were in the clouds but later realized "unconventionally" his intellectual passion was actually in what lies underground. While working full time and attending UT he was promoted to Operations Manager at Albertsons, and made a career of it for 15 years. He graduated in 2008 with a Bachelor's in History and successfully completed the UT Business Foundations Program. In 2011, he began pursuit of his passion in Geology and the Petroleum Industry and was ultimately accepted into the Master of Science Geology program at The University of Texas at El Paso in 2014.

Andre was one of the five members that participated in the 2016 American Association of Petroleum Geologists (AAPG) Imperial Barrel Award (IBA) global competition where his team was awarded 1st place World Champions out of 176 Universities. In May of 2017 he completed his Bachelor of Science Geology degree and also took an internship with Chesapeake Energy in Oklahoma City working within the Gulf Coast Exploration Team. In the fall of 2017 he accepted an offer from Halliburton where he will be working as a petroleum engineer after defending his Master's thesis.

Email: andrellanos10@gmail.com

This thesis was typed by the author, Andre Armando Llanos.